Equatorial ionosphere responses to two magnetic storms of moderate intensity from conjugate point observations in Brazil

M. A. Abdu,[1] I. S. Batista,[1] F. Bertoni,[2] B. W. Reinisch,[3,4] E. A. Kherani,[1] and J. H. A. Sobral[1]

Received 19 September 2011; revised 22 March 2012; accepted 6 April 2012; published 19 May 2012.

[1] Equatorial ionospheric responses during two magnetic storms of moderate intensity are investigated, for the first time, by conjugate point observations in Brazil. The study focuses on storm-induced changes in the evening prereversal vertical drift, thermospheric trans-equatorial winds, spread F/plasma bubble irregularity development, electron density/plasma frequency heights, the EIA strength, and zonal plasma drifts. It is based on data obtained from five Digisondes operated in Brazil, three of them being part of a conjugate point equatorial experiment (COPEX) involving a dip equatorial and two magnetic conjugate sites at $\pm 12^{\circ}$. The other two were operated at the equatorial ionization anomaly (EIA) trough and crest locations at nearby magnetic meridians. The results bring out, and clarify, many outstanding aspects of the strong influence of storm time electric fields on the equatorial ionosphere at different phases of the two long lasting storm sequences. During both storms prompt penetration electric fields dominated the ionospheric response features as compared to the disturbance wind dynamo effects that were not very conspicuous. An under-shielding (over-shielding) electric field occurring in the evening hours causes enhancement (suppression) of the prereversal vertical drift and post sunset spread F/plasma bubble generation. The same electric fields cause post sunset EIA enhancement and suppression, respectively. Post sunset (post midnight) spread F can develop from under-shielding (over-shielding) electric fields, while it can be disrupted by over-shielding (under-shielding) electric field. Trans-equatorial winds are found to be ineffective to stabilize the post sunset F region against the destabilizing effect of strong prereversal vertical drift. Storm time westward plasma drifts are found to be driven by prompt penetration eastward electric fields (through their effect of inducing vertical Hall electric fields), rather than by a disturbance westward thermospheric wind during these storms.

Citation: Abdu, M. A., I. S. Batista, F. Bertoni, B. W. Reinisch, E. A. Kherani, and J. H. A. Sobral (2012), Equatorial ionosphere responses to two magnetic storms of moderate intensity from conjugate point observations in Brazil, *J. Geophys. Res.*, *117*, A05321, doi:10.1029/2011JA017174.

1. Introduction

[2] Ionospheric responses to magnetic storms are manifestations of rapid changes in the interactive processes operating in the magnetosphere- ionosphere-thermosphere system as a result of sudden injection of solar wind energy into the system. A southward turning of the interplanetary magnetic field Bz initiates the onset of a substorm marked by sudden increase in the auroral electroject activity (AE) as its growth phase that is followed by a recovery phase, the sequence repeating a few times during a typical magnetic storm (for information, see, e.g., *Rostoker et al.* [1980], *Fejer* [1986], and *Gonzalez et al.* [1994]). The Dst variations that accompany (often starting with an SSC increase) presenting a main phase decrease and a recovery phase represent the storm evolution over middle and low latitudes [e.g., *Akasofu and Chapman*, 1972]. The degree of the Dst main phase decrease is a measure of the intensity of a storm, characterized as intense/super, moderate, and weak for the Dst < -100 nT, -100 nT $<$ Dst < -50 nT, and -50 nT $<$ Dst < -30 nT, respectively. In recent years numerous papers have discussed the drastic modifications suffered by the equatorial to midlatitude ionosphere during several intense/super storms that occurred during the last solar activity cycle [e.g., *Abdu et al.*, 2003, 2007; *Maruyama et al.*, 2004; *Tsurutani et al.*, 2004; *Mannucci et al.*, 2005; *Lin et al.*, 2005; *Sahai et al.*, 2005; *Zhao et al.*, 2005; *Batista et al.*, 2006; *Basu et al.*, 2007; *Paznukhov et al.*, 2009; *Horvath and Lovell*, 2010]. Some previous studies on the equatorial

[1]Instituto Nacional de Pesquisas Espaciais, São José dos Campos, Brazil.
[2]CRAAM, Mackenzie University, São Paulo, Brazil.
[3]Lowell Digisonde International, LLC, Lowell, Massachusetts, USA.
[4]Center for Atmospheric Research, University of Massachusetts, Lowell, Massachusetts, USA.

Corresponding author: M. A. Abdu, Instituto Nacional de Pesquisas Espaciais, Av. dos Astronautas, 1758 Jardim da Granja, 12201-970 São José dos Campos, SP, Brasil. (maabdu@dae.inpe.br)

0148-0227/12/2011JA017174

ionospheric responses to storms of varying intensities are also of relevance here [see, e.g., *Sobral et al.*, 1997; *Sastri et al.*, 2000, and references therein]. In contrast to the extensive coverage of major storms that produce often spectacular response features in the ionosphere, there has been little discussion on the ionospheric responses to moderate intensity storms over low latitude which is the focus of this paper (for some limited results in this respect, see, for example, *Sastri et al.* [1997], *Tulasi Ram et al.* [2008], and *Sreeja et al.* [2009]). Irrespective of the storm intensity the same general description is valid for the sequence of storm phases responsible for the modifications of the low latitude ionosphere-thermosphere system.

[3] Storm time electric fields are a major source of ionospheric modification over equatorial and low latitudes. During a storm/sub storm development under the Bz south condition the polar cap dawn-dusk electric field promptly penetrates to equatorial latitudes until it is partially balanced by the development of a shielding layer (by the region 2 field aligned current) that develops in time scales of approximately half an hour to several hours [see, e.g., *Kelley et al.*, 1979; *Fejer et al.*, 1990; *Kikuchi et al.*, 2000]. The prompt penetrating electric field, that is, the under-shielding electric field, is eastward (westward) on the day (night) side of the equatorial ionosphere, with the polarity reversed for the over-shielding electric field that occurs at the sub storm recovery phase. (For simplicity of discussion from here on we may use the acronym PPEF for Prompt Penetration Electric Field, which is the under-shielding electric field, whereas the over-shielding electric field, which simply is a penetration electric field, may be denoted as PEF). Under extended AE activity with Bz southward fluctuations, an imperfectly shielded penetration electric field of longer duration can dominate the low latitude ionosphere [see, e.g., *C.-S. Huang et al.*, 2005; *Abdu et al.*, 2007; *Wei et al.*, 2008]. The ionospheric conductivity longitudinal gradient (especially, at the sunset and sunrise terminators) can enhance the penetration electric field intensity. As a result, the PPEF has its maximum eastward (westward) intensity at post sunset (pre sunrise) local times, as observed, for example, from analysis of ROCSAT 1 vertical plasma drift data by *Fejer et al.* [2008] and from global general circulation simulation studies by *Richmond et al.* [2003] [see also *Maruyama et al.*, 2011]. It is also well known that the global thermospheric disturbances originating from auroral heating could produce long duration disturbance wind dynamo electric fields (DDEF) [*Blanc and Richmond*, 1980] that dominate the low latitudes with a delay of ~6 h from the first incidence of the PPEF following a storm onset. Numerical simulation predicts thermospheric wind surges over low latitude within only 2–3 h from the storm energy input at high latitudes [*Fuller-Rowell et al.*, 2002]. The disturbance wind dynamo electric field that follows the over-shielding electric field may last from several hours up to one day [*Scherliess and Fejer*, 1999] and have a polarity local time dependence that is nearly opposite to that of the under-shielding PPEF [*Richmond et al.*, 2003; *Fejer et al.*, 2008; *C.-M. Huang et al.*, 2005]. From coupled model simulations involving interactive feedbacks through electrodynamic processes in the magnetosphere-plasmasphere-ionosphere-thermosphere system, *Maruyama et al.* [2011] have shown that the storm time equatorial electric fields are the results of nonlinear interaction between the PPEF and DDEF. In other words the intensity and local time patterns of either of these electric fields identified as such would depend upon the response of a preconditioned coupled system. Such interactive response is however more significant in the case of super storms as pointed out by these authors.

[4] During intense storms the PPEF of eastward polarity can cause large uplift of the ionosphere in the day and evening sectors resulting in large increases of the total electron content (TEC) of the EIA as observed by GPS receivers, ionosondes and other techniques [*Batista et al.*, 1991; *Abdu*, 1997; *Tsurutani et al.*, 2004; *Maruyama et al.*, 2004; *Lin et al.*, 2005; *Basu et al.*, 2007; *Abdu et al.*, 2008]. The EIA can expand in latitude with the ionization crests of enhanced intensity displaced to midlatitudes [*Abdu*, 1997; *Mannucci et al.*, 2005] accompanied by large-scale equatorial TEC depletions [*Greenspan et al.*, 1991; *Basu et al.*, 2001]. The penetration eastward electric field can cause large enhancement in the vertical plasma drift at the low latitude dusk sector where the prereversal enhancement in eastward electric field (PRE) due to the F layer dynamo is normally active. This can also cause enhanced instability growth by the Rayleigh-Taylor mechanism leading to development or intensification of equatorial spread F irregularities (ESF) even during seasons of low PRE intensity and therefore minimal ESF occurrence [*Abdu et al.*, 2003; *Li et al.*, 2010]. Alternatively, a large westward electric field in the dusk sector originating from over-shielding process associated with Bz northward turning and/or AE recovery, or from a disturbance wind dynamo can cause suppression of plasma bubble development [*Abdu et al.*, 2009a]. While these observational results were generally derived from studies of major/intense storms, little is known about the corresponding response features during storms of moderate intensity. The latter information is especially important for a better understanding of the nature of the dependence of the low latitude ionospheric response (in terms of any of the above mentioned features, EIA, plasma bubbles, etc.) on the driving storm energy input into the ionosphere-thermosphere system as measured by the associated AE and Dst intensities.

[5] This question has motivated the present case study on the responses of the equatorial - low latitude ionosphere over Brazil during two magnetic storms of moderate intensity (with maximum Dst decrease of 80–100 nT) that occurred on 24 October and 20 November 2002 during the COPEX-2002 campaign period (for more information on the Conjugate Point Equatorial Experiment (COPEX) Campaign and related results, see, for example, *Abdu et al.* [2009b], *Batista et al.* [2008], *Reinisch et al.* [2004], and *Sobral et al.* [2009]. For the first time, we present and discuss here observations at magnetic conjugate sites that permit identification of some unique features of the low latitude storm time responses that are otherwise unachievable. Data simultaneously registered by Digisondes at five sites in Brazil are analyzed. Table 1 shows the coordinates of these stations and Figure 1 shows their locations. Three of them constituted the COPEX sites with Campo Grande and Boa Vista forming the South and North conjugate sites, to be identified also as Seq (South of equator) and Neq (North of equator), respectively, and Cachimbo near the dip equator. The magnetic field lines of the conjugate point E layers mapped to the dip equatorial F layer bottom-side near 350 km. The two other sites are

Table 1. Coordinates of the Stations Used in the Analysis

Coordinates	Station Name				
	Cachimbo	Boa Vista	C. Grande	São Luis	C. Paulista
Latitude (deg)	9.5 S	2.8 N	20.5 S	2.6 S	22.7 S
Longitude (deg)	54.8 W	60.7 W	54.7 W	44.7 W	45 W
Dip angle	−4.2	22.0	−22.3	−3.85	−33.7
Magnetic latitude	−2	11	−11	−1.6	−16
Declination	−16.7	−14	−15.1	−20.7	−20.6

Sao Luis, very close to the dip equator, and Cachoeira Paulista, at the southern EIA crest, at nearby magnetic meridians displaced eastward of the COPEX meridian by 10–15°. The F layer heights at successive plasma frequencies, the layer peak characteristics, hmF2 and foF2, the range spread F, the inferred trans-equatorial winds, and the vertical and zonal plasma drifts are analyzed in an attempt to determine their response features at different phases of these moderate intensity storms. Specific focus is given to the conditions governing the developments/suppression of the evening prereversal enhancement in the vertical drift (PRE), the post sunset and post midnight spread F developments, the equatorial ionization anomaly (EIA) dynamics, and the zonal plasma drift due to Hall conduction. The conjugate points observations have made possible, for the first time, an assessment (at least partially) of the competing roles of the storm time disturbance zonal electric fields and the meridional/trans-equatorial winds in the processes leading to the development/ suppression of the post sunset spread F/plasma bubble irregularities.

2. Presentation of the Results

2.1. The Moderate Intensity Storm of 24–27 October 2002

[6] Figure 2 shows one-minute resolution magnetic indices, that is, the IMF Bz, the auroral electrojet activity AE and the SYM-H representing the Dst, and the 3-hourly Kp values, during 23–26 October 2002. The storm effectively started at 00:00 UT of 24 October 2002 as indicated by the IMF Bz southward turning, with simultaneous rapid intensification of the AE, and the Dst decrease, that set in at this time (arrow 1). The maximum deviations in the Bz, AE, and Dst during the event sequences that followed were of the order of −10 nT, 1200 nT, and −80 nT, respectively. In order to have an idea of how moderate this storm event was, one can compare these values with the corresponding values that characterized the widely investigated super storm of October 29–30, 2003 that were, respectively, −35 nT, 5000 nT, and −400 nT [see, e.g., *Zhao et al.*, 2005; *Abdu et al.*, 2007]. Thus, assuming a gross linear dependence of the magnetic indices on the storm energy input we might note that in the present storms the energy input can be approximately a factor of 4–5 weaker than in the case of a typical super storm. The degree of ionospheric response to a moderate intensity storm such as this one is not expected to be spectacular as it can be for a super storm, and hence an evaluation of the responses in this case clearly demands very careful scrutiny of the data. In Figure 2 we may note large degree of fluctuations in Bz, with predominantly southward polarity during the first one and half days (from the storm onset), with a few episodes of northward turnings. The southward (northward) excursions of Bz appear generally well correlated with the intensification (recovery) of the AE and Dst of which clear examples can be noted at 00 UT on 24 October/21 LT on 23 October, 12 UT/09 LT, and 21 UT/18 LT on 24 October (indicated by the arrows 1, 2, and 4, respectively). The Bz turning north at sunset (arrow 4) has potentially significant impact on the PRE and spread F developments, which will be discussed later. Starting at this time (18 LT on 24 Oct.) the Dst presented a slow recovery with some superimposed activities in AE and Bz. The slow growth and recovery of the storm is reflected also in the accompanying Kp variations.

[7] The F layer true heights over the COPEX sites for successive plasma frequencies (from 3 MHz upward at 1-MHz increments till foF2) are presented in Figure 3, for the entire storm interval. The corresponding F layer peak height hmF2 is compared with its quiet time patterns in Figure 4. (We may point out here that in the presence of spread F traces the scaled hmF2 values can be uncertain to a certain degree depending upon the intensity of the range spreading and on the multiple traces that might be present. This factor has been taken into account in our interpretation of the relevant results.) Also shown in this figure are the spread F intensities over the three sites represented by the parameter, fop, the top frequency of the range spread F trace in the ionogram. A comparison of the F layer heights over the conjugate sites shows that they are generally higher (with a few exceptions), with larger separation among the iso-lines, over Seq than over Neq (on all the four days plotted in Figures 3 and 4). This would suggest the presence of trans-equatorial wind blowing predominantly from the southern to the northern hemisphere during this period. We further note that the height oscillations over the conjugate sites differ significantly from those over the equator, that

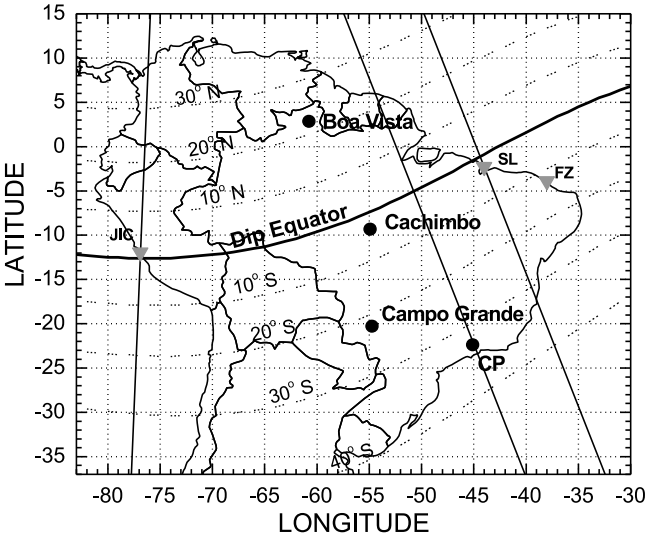

Figure 1. Map showing the Digisonde sites. The COPEX Digisonde sites are: Boa Vista, northern conjugate point; Campo Grande, southern conjugate point; and Cachimbo close to the magnetic equator. Also marked are the locations of the permanent Digisonde stations in Brazil, Sao Luis (SL), Fortaleza (FZ), and Cachoeira Paulista (CP).

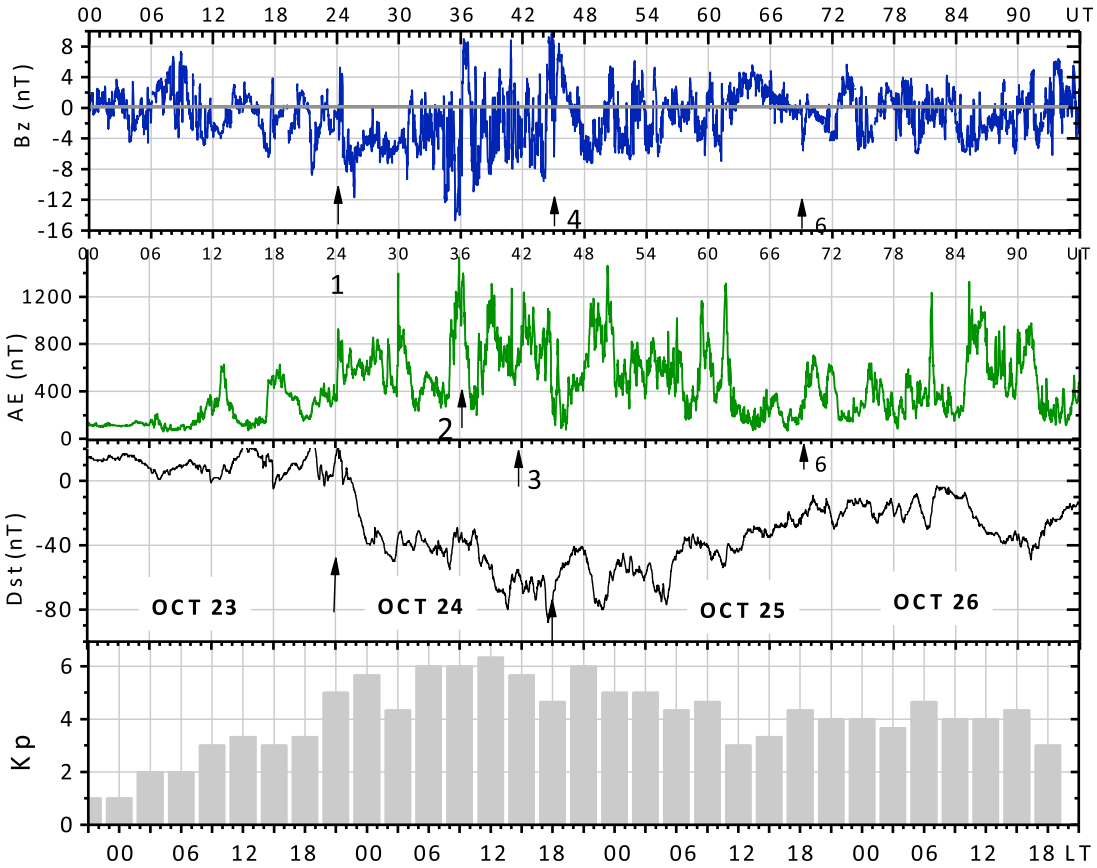

Figure 2. Variations in the magnetic indices during the moderate storm that started at 00 UT of 24 October (21 LT of 23 Oct) 2002. The one-minute indices are: the IMF Bz from ACE satellite (first panel), the auroral activity AE index (second panel), and the SYM-H/Dst (third panel); and the 3-h planetary index Kp (fourth panel). (The numbered arrows 1, 2 etc., indicate the features at different LT/UTs discussed in the text, and they have the same numbering in Figures 2, 3, 4, 5 and 7.) Note that we have used the 45°W meridians Brazilian standard time as LT in all the figures.

may be caused by the presence of gravity waves, some of which present downward phase progression characteristics as indicated (for example, near 13 LT on Oct 24, in Figure 3) by the vertical slant lines cutting the iso-lines at both the Neq and Seq. The height oscillations are also asymmetric at the conjugate sites suggesting a certain degree of hemispheric difference in the wave characteristics, which may arise from trans-equatorial winds (for the role of trans-equatorial winds on F layer heights, see *Abdu et al.* [2009b]).

[8] We may examine in the results in Figures 3 and 4 the F layer height response to storm time electric fields based on the local time dependence of such electric fields as predicted by some leading observational/simulation studies. From analysis of ROCSAT-1 data *Fejer et al.* [2008] presented longitudinally averaged equatorial prompt penetration vertical plasma drifts (eastward electric field) near 600 km that corresponded to a step function increase in the AE index by 300 nT (their Figure 1). The Magnetosphere-Thermosphere-Ionosphere-Electrodynamics General Circulation Model (MTIEGCM) simulation results by *Richmond et al.* [2003], which corresponded to the end of a long lasting storm representing imperfectly shielded PPEF (their Figure 4), shows excellent agreement with the PPEF vertical drift local time variation presented by *Fejer et al.* [2008]. The PP vertical drift in Fejer et al. peaked at 1830 LT with 5–15 m/s depending upon the season (see their Figure 1), and then decreased rapidly reversing to downward (westward electric field) near midnight. At 2100 LT (0000 UT), which is the storm onset time in our case, the PPEF vertical drift is about 20 percent of the peak value (or even less, depending upon the season). Thus we expect only a 'small' change in the vertical drift, or in the F layer heights, due to the PPEF associated with the storm onset at 21 LT (0000 UT), which indeed seems to be the case as judged by the very small height change/increase over Cachimbo at this time in Figures 3 and 4. At the conjugate sites, with magnetic inclination of $\pm 23°$, an additional factor in the height response is the dominating influence of thermospheric meridional wind, which could mask any response.

[9] Here we need to point out that two important factors need to be considered while examining the response of the vertical drift, or the F layer heights, to disturbance electric fields in all the data analyzed here. They are: 1- the response of the radio wave reflection heights (as sensed by the Digisonde) to changes in zonal electric field becomes less efficient under the dominating influence of the daytime photochemistry which is height dependent, and 2- the

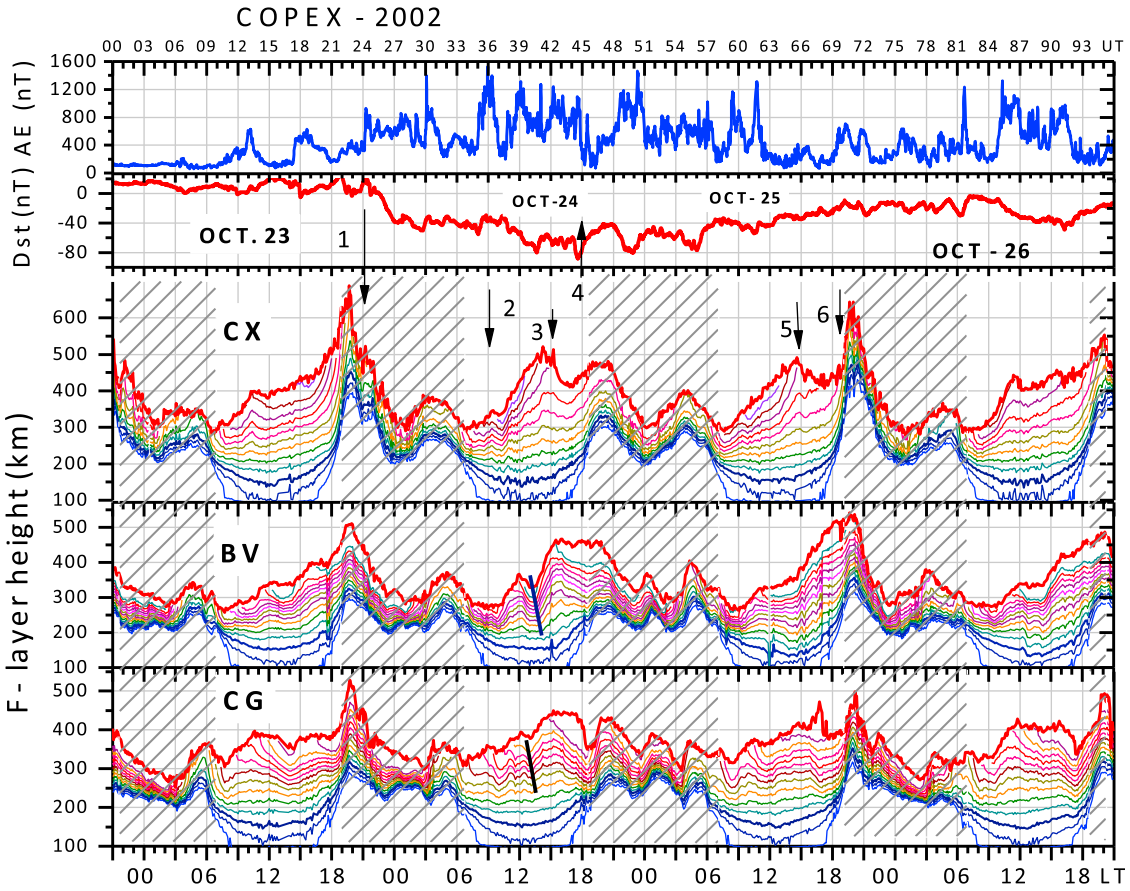

Figure 3. On four days covering the 24 October 2002 storm are shown: the magnetic activity indices AE and Sym-H (Dst) (first and second panels); the F layer heights at plasma frequencies in step of 1 MHz, from 3 MHz till foF2, and the hmF2, over the COPEX sites: Cachimbo (CX) near the magnetic equator and Boa Vista (BV) and Campo Grande (CG), the north and south conjugate sites, respectively. Local time scale is shown at the bottom, and UT is shown at the top. Night hours are shown shaded.

penetration efficiency of the storm time electric fields is strongly local time dependent. Near evening and night hours and for heights >300 km the factor 1 has minimal effect so that the vertical drift as measured by the Digisonde closely approaches the real vertical plasma drift [see, e.g., *Bittencourt and Abdu*, 1981]. During daytime the photochemistry influence on the height variations decreases with increasing height so that the measurement sensitivity of the response to PPEF improves for larger F layer heights [see, e.g., *Balan et al.*, 2011].

[10] With the Bz turning north and the AE recovery at ~3600/1200 UT (0900 LT) on 24 October, indicated by the arrow 2 in Figure 2, we notice in Figures 3 and 4 the effect of an over-shielding electric field of westward polarity in the form of a clear, although very small, reduction in hmF2 over Cachimbo (also indicated by the arrow 2). Again, as in the case of the PPEF (at 0000 UT discussed above), there was no perceivable effect at the conjugate sites (for reasons mentioned above). Here we may point out that the westward polarity of the over-shielding electric field (PEF) indicated by the 0900 LT hmF2 decrease is consistent with the polarity local time dependence of this electric field which is exactly opposite to that of the PPEF [*Fejer et al.*, 2008]. During the following period of ~6–7 h (that is, ~1030 LT – 17 LT), the Bz was predominantly southward with large AE intensifications. As a result, the associated PPEF appears to be responsible for the rise in hmF2, clearly observed over Cachimbo, that was interrupted at 1500 LT indicated by the arrow 3 (in Figure 4 the rise in hmF2 and the reversal can be clearly seen over Cachimbo with respect to the quiet day curve). With the Bz marginally south and AE beginning a slow recovery this hmF2 decrease over Cachimbo indicates a westward electric field that can be taken for an over-shielding effect. The over-shielding electric field intensified with the more rapid AE recovery when Bz turned north (arrow 4 in Figure 2). This situation must have contributed to the suppression of the PRE, which is well illustrated in the vertical plasma drift variation to be described in Figure 5. With the reduced PRE the spread F development was totally suppressed on this evening as can be noted in Figure 4. The possibility as to whether or not these effects could as well have been caused by a westward disturbance wind dynamo (DD) electric field will be examined in section 3.4.

[11] It needs mentioning that the vertical plasma drift velocity analyzed in this paper was in part calculated as the time rate of change of the F layer true heights, d(hF)/dt, at specific plasma frequencies as obtained from the SAO software of the Digisonde system [*Reinisch*, 1996; *Reinisch*

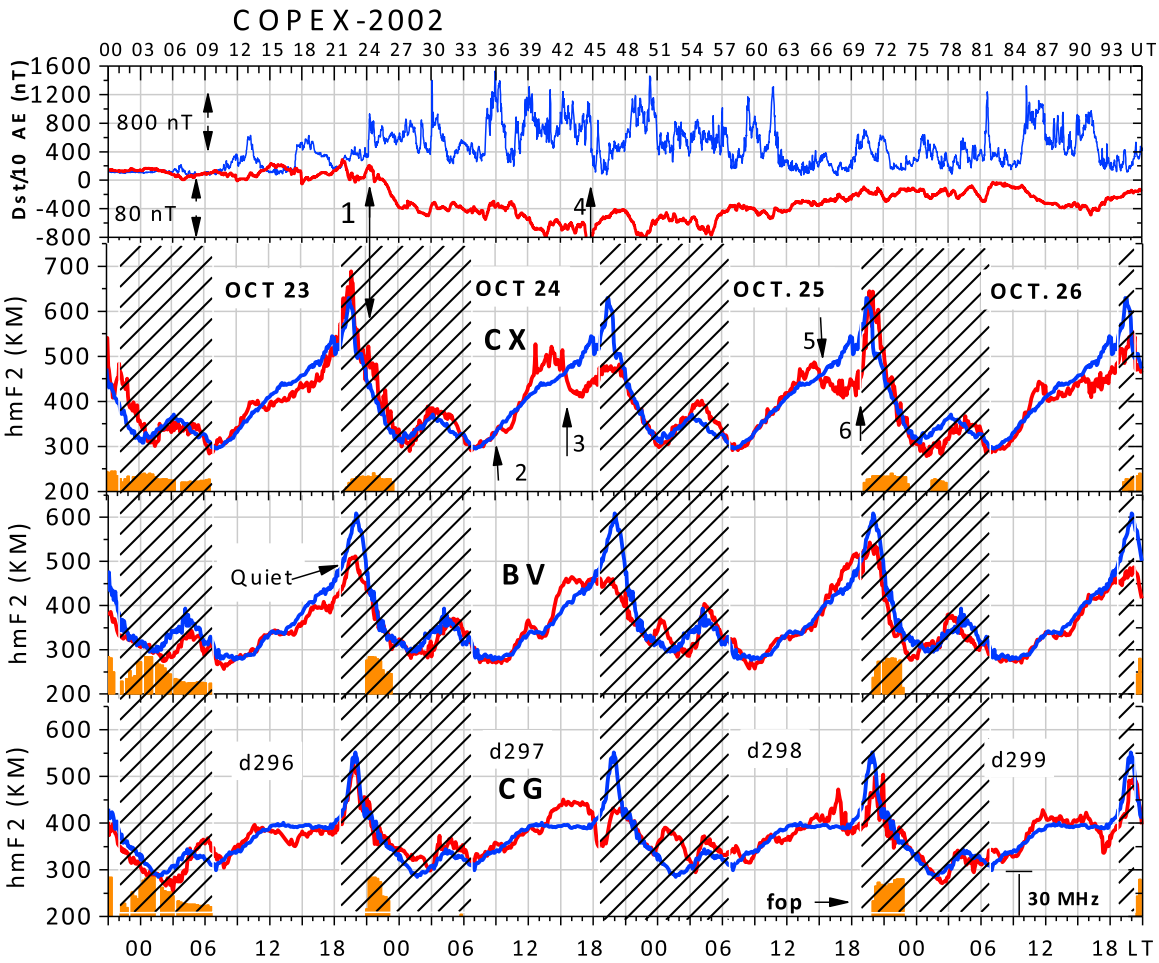

Figure 4. The AE and Dst variations during the 24 October storm (first panel). The F layer peak height (hmF2) over Cachimbo (CX), Boa Vista (BV), and Campo Grande (CG) (second through fourth panels). The individual day plots are in red and the quiet day reference in blue. The spread F intensity is plotted as orange histograms using the parameter fop (the top frequency of the spread F trace) which can be read from the *y* axis as fop = (y-200)/3. A vertical scale is shown by a bar representing fop = 30 MHz. Night hours are shown shaded.

et al., 2009; *Khmyrov et al.*, 2008]. The velocities so obtained are comparable with the vertical velocity calculated from the sky map/drift mode operation of the Digisonde with the utilization of the Drift Explorer software [*Kozlov and Paznukhov*, 2008]. It has been shown from theoretical calculations [*Bittencourt and Abdu*, 1981] and experimental validation [*Scali et al.*, 1995] that such velocities are identical to the vertical plasma drift velocities, for F layer heights near and above 300 km where the recombination effect becomes negligible, and the photo-chemistry does not dominate.

[12] Figure 5 shows, in the successive panels, the spread F occurrence start times at the COPEX sites, the vertical drift over Cachimbo, the parameter $\mathrm{dhmF2}_{(\mathrm{CG-BV})}$, and the AE and Dst indices. The parameter $\mathrm{dhmF2}_{(\mathrm{CG-BV})}$ is the hmF2 difference between the conjugate sites, which is a measure of the trans-equatorial wind (TEW) as was discussed recently also from COPEX results by *Abdu et al.* [2009b]. Notice that this parameter presents a negative increase near the sunset hours on 24 October, and on the following two days, which suggests an enhanced intensity of the TEW as compared to the previous evening as well as to its quiet time pattern (also shown in the figure). The TEW increase is directed southward at the time of the PRE. Any possible connection between the enhanced TEW and the suppression of the ESF (or the PRE) that occurred on this evening will be discussed in section 3.2.

[13] Continuing with the description of the event sequence, we may wonder whether the minor hmF2 increase in the pre sunrise-morning hours of 25 October over Cachimbo (Figure 4) could be indicative of a weak eastward DDEF effect. However, the ongoing AE activity accompanied by Bz transients at the same time (Figure 2) does not allow such identification. Similar considerations hold for what looks like a westward DDEF effect (height decrease) that occurred near 15 LT on the same day and near the same local time on the previous and next days. On the other hand, the near complete recovery of the AE activity by 1700 LT on 26 October, some two hours before the PRE, might possibly argue for a DDEF of westward polarity to be a cause of the reduced PRE intensity that followed (see also Figure 5).

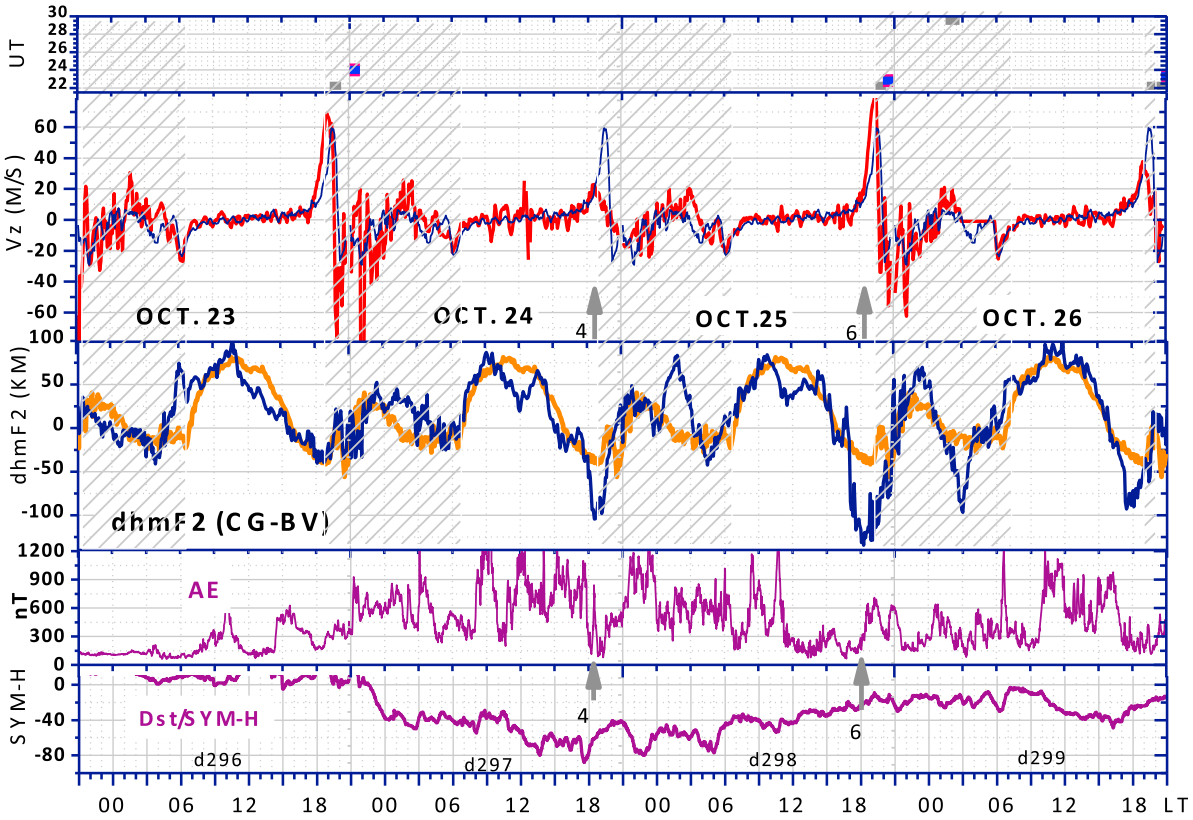

Figure 5. The spread F starting time in LT and UT at Cachimbo (gray), Boa Vista (pink) and Campo Grande (blue) (first panel); the F layer vertical drift over Cachimbo for individual days (red) and the reference quiet day curve (blue) (second panel); the parameter dhmF2(CG − BV) on individual days (blue) and reference day (orange) (third panel); and the Indices AE and SYM-H/Dst (fourth and fifth panels).

[14] An outstanding feature that calls our attention is the rapid increase in the heights on the evening of 25 October starting near 1830 LT right at the time of the PRE as can be seen in Figures 3 and 4 (arrow 6). A large eastward electric field, which is now superimposed on the background PRE, caused a vertical drift of 80 m/s (see Figure 5). This can be identified as a PPEF associated with an AE intensification (by about 600 nT), under a brief Bz southward turning, that occurred at this time (see Figure 2). As a result, ESF development occurred at all the three COPEX sites (Figure 4) indicating topside bubble growth. The ESF developed also over the other sites Sao Luis and Cachoeira Paulista to be described in Figure 7.

[15] The storm that was in its recovery became active again beginning in the forenoon hours of 26 October with the Dst and AE presenting renewed activity under Bz south conditions, and the F layer heights (Figures 3 and 4) presented fluctuations due to the associated PPEF. The lower than quiet time F layer heights, later on this day, as seen in Figures 3 and 4, might arise largely from an over-shielding westward electric field associated with the AE recovery, which occurred near 1630 LT. The PRE that followed was of small amplitude (only 35 m/s, Figure 5), perhaps due to a DDEF (as mentioned before), but it appears sufficient to cause bubble development (Figure 4) with a very slow rise velocity as judged from the spread F occurrence at the conjugate sites that was more delayed as compared to the previous evening. Further, the spread F that began over SL did not develop fast enough to be observed over CP till 21 LT (the end of the data) as may be noted in Figure 7 (to be described later).

[16] Figures 6 (left) and 6 (right) show the vertical plasma drift, Vz, and zonal plasma drift, Vx, respectively, as obtained from the Digisonde drift explorer software from 09 to 09 LT on 24–25 October 2002 for the three COPEX sites. The drifts are compared with their quiet day values shown as the reference (blue) curve. The prereversal vertical drift with reduced amplitude over Cachimbo (shown also in Figure 5) is significantly more suppressed over the two conjugate sites. The degree of the suppression is asymmetric, with the peak Vz over the Neq (near 19 LT) being greater than that over the Seq by ~10 m/s, that is, $\Delta V_{zp(CG\text{-}BV)} = -10$ m/s. This would suggest the presence of a southward-directed trans-equatorial wind as suggested also by the negative deviation in the $dhmF2_{(CG\text{-}BV)}$ at this time in Figure 5. By using the relationship: $\Delta V_{zp(CG\text{-}BV)} = (U_{mmCG} + U_{mmBV})\cos(I)\sin(I)$, we can determine the value of TEW as ~30 m/s southward, which is consistent with that suggested by the value of $dhmF2_{(CG\text{-}BV)} \approx 50$ km in Figure 5 (for more details, see *Abdu et al.* [2009b]). In the above equation U_{mm} represents the magnetic meridian wind with the subscripts CG and BV for Campo Grande and Boa Vista, respectively, and I being the dip angle. Any consequence of this TEW on ESF development will be discussed in section 3.2.

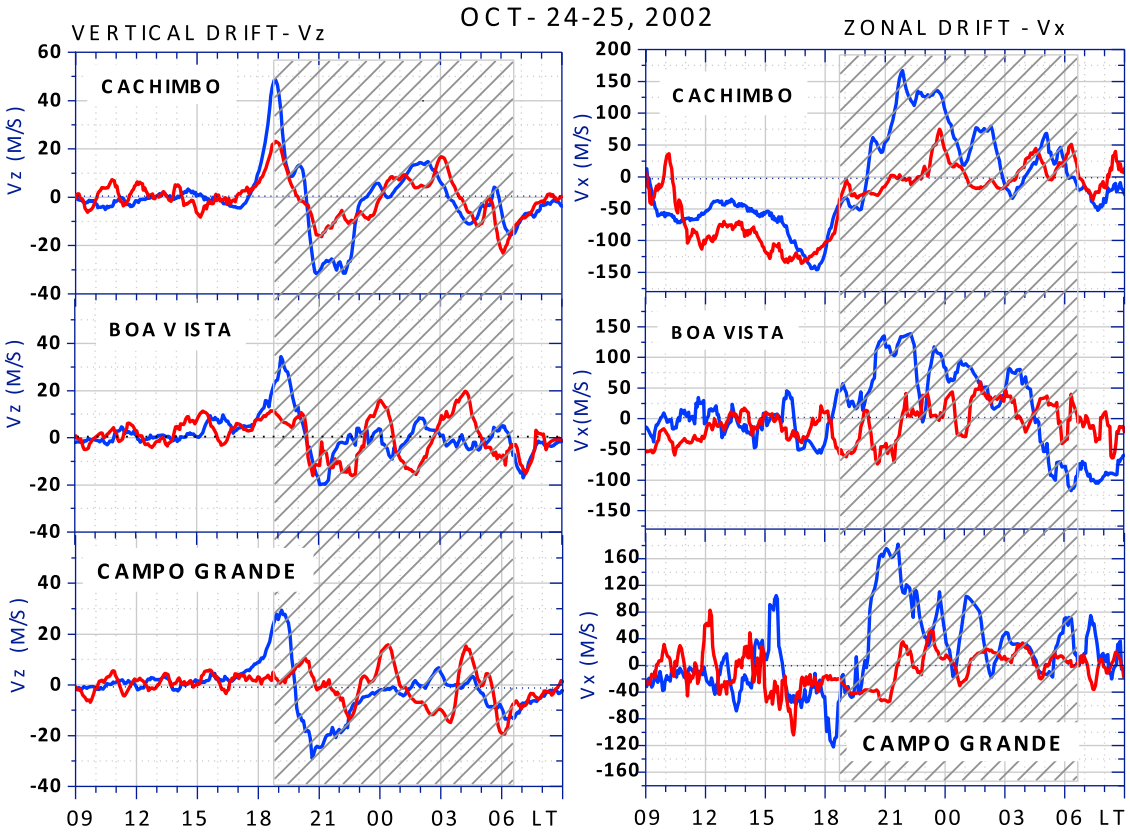

Figure 6. The F layer (left) vertical drift and (right) zonal drift for (top) Cachimbo, (middle) Boa Vista and (bottom) Campo Grande plotted on 24–25 October 2002. Night hours are shown shaded. The quiet day curve is in blue and the disturbed day is in red.

[17] The zonal plasma drift over the three sites plotted in Figure 6 (right) shows that the quiet time drift (blue curve) is generally westward during the day and eastward during night. The eastward drift velocity peak that occurs near 21 LT is of the order of 150 m/s. For the mean solar flux condition (F10.7 = 165) that characterized the COPEX period this peak drift and its local time are very consistent with those of the Jicamarca average zonal plasma drift for similar solar flux conditions [*Fejer et al.*, 1991]. The time of the evening drift reversal to eastward appears to be a bit delayed (by 1–2 h) over the COPEX sites (measured by Digisonde) as compared to the zonal plasma drift reversal time over Jicamarca (measured by incoherent scatter radar), or the ion zonal velocity reversal time measured by the DE2 satellite by *Coley et al.* [1994] which usually occurs near 17 LT. This time delay may be attributed to factors such as the differences in the height domains and the plasma characteristics sampled by the different techniques. For example, a westward drift enhancement is clearly noticeable near sunset over Cachimbo (Figure 6), which appears to contribute to (or cause) the delay in the drift reversal time. Such westward drift occurring at the F layer bottomside, as sensed by the Digisonde, could as well be part of the evening plasma vortex flow discussed by *Kudeki and Bhattacharyya* [1999]. We do not intend to further discuss this point here. The disturbance drift (red curve) shows significant deviations from the quiet time drift, the early nighttime eastward drift tending to reverse to westward being a notable feature at all the three sites. A westward increase in the drift in the afternoon hours over Cachimbo may especially be noted. An interpretation of this disturbance variation in zonal drift will be presented in section 3.4.

[18] The responses to this storm at a more eastern longitude (by 10° from the COPEX longitude) as observed by the Digisondes at Sao Luis and Cachoeira Paulista are presented in Figure 7 wherein the plasma frequency isoline plots are similar to those of Figure 3. Spread F intensity is plotted as in Figure 4. Additionally we compare the hmF2 and foF2 values over SL (at the EIA trough) with those over CP (at the EIA crest), which permits an evaluation of the EIA response to the storm. We may notice that the F layer responses over SL during the storm sequences are very similar to that over Cachimbo in Figure 3 (though there are data gaps on 25 October during 16–19 LT over SL and during 1930- 22 LT over CP where the SF occurrence sequence was interrupted). In this respect the following major features (indicated by arrows) may be noted: The small height increase, followed by a rapid decrease, at the start of the storm (AE intensification with Bz south) at 0000 UT/2100 LT on 24 October are identical at both locations (as to be expected). So are the hmF2 decrease (indicated by arrow 3 in Figures 3 and 7) and the evening vertical drift (PRE) suppression (arrow 4, Figures 4, 5, and 7) that are apparently caused by an overshielding electric field as suggested by the AE decreases at these times. We may note in the fifth panel of Figure 7 large

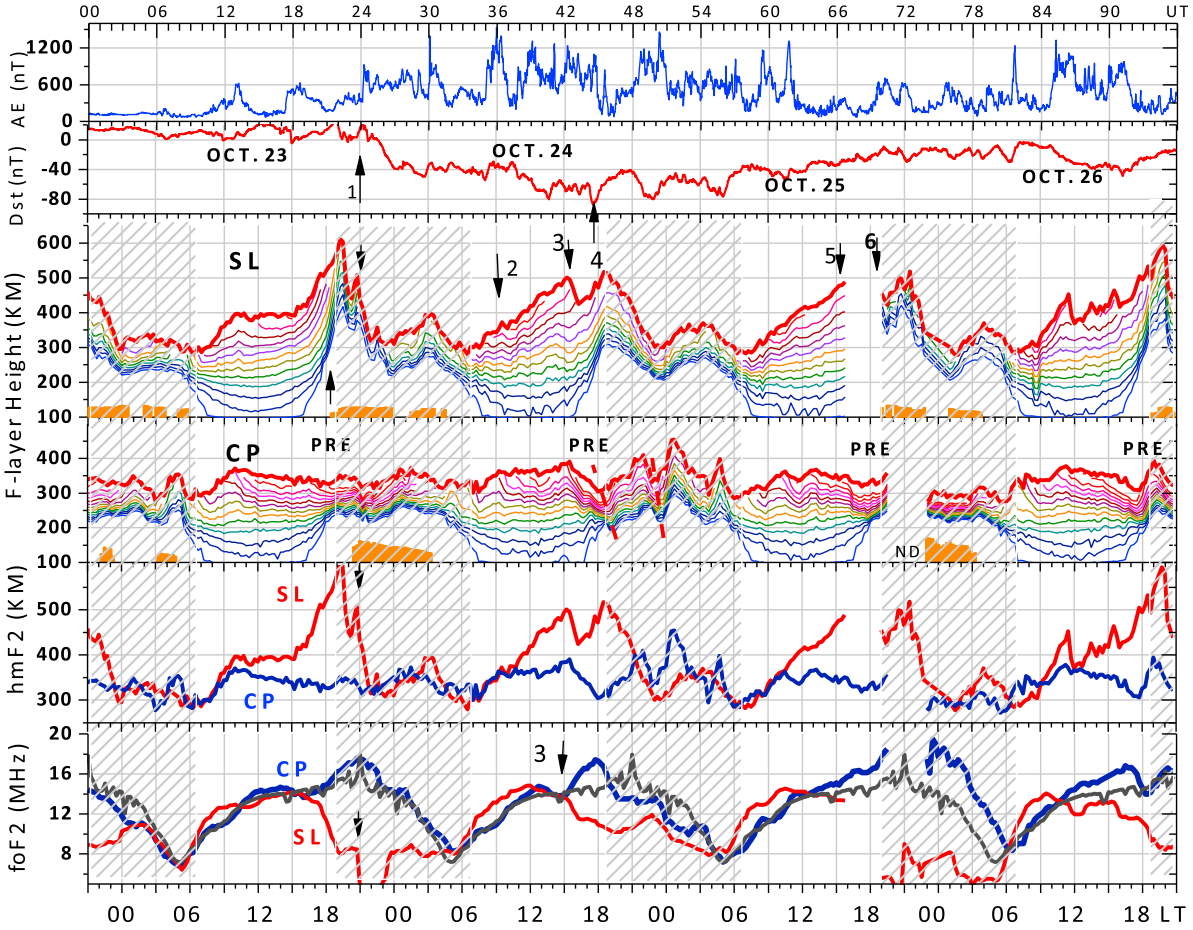

Figure 7. On four days covering the 24 October 2002 storm are shown: the one-minute resolution magnetic activity indices AE and Sym-H (Dst) (first and second panels), the F layer heights at successive plasma frequencies from 3 MHz increasing in step of 1 MHz till foF2, and the hmF2, over Sao Luis (SL) and Cachoeira Paulista (CP) respectively (third and fourth panels), a comparison of the hmF2 over SL and CP (panel 5), and a comparison of the foF2 over SL and CP (sixth panel). Over CP the blue curve represents the foF2 on the individual days and the foF2 reference curve (mean of four quietest days of the period) is shown in gray. Local time scale is shown at the bottom and UT scale at the top. The spread F intensity (orange histograms) is plotted in terms of the parameter fop (the top frequency of the spread F trace) given by fop = (y-200)/3, where y is the value on the *y* axis. The vertical scale for fop is the same as that shown in Figure 4. Night hours are shown shaded. There is no data during 1530–1800 LT and 1915–2245 LT over SL and CP, respectively.

differences in the hmF2 values between SL and CP during daytime and evening hours. The generally smaller hmF2 values over CP are in part due to the equatorial zonal electric field vertical structure (decreasing with height) and the lower vertical plasma drifts (also due to the magnetic field line inclination being −36°) over this station. Additionally the meridional wind that has little influence on the F layer heights over SL strongly controls the hmF2 fluctuations over CP. Differences in foF2 between the two sites, which is a measure of the EIA strength, can also be noted and it is large in the afternoon-evening hours during the storm period (sixth panel). A comparison of the foF2 of the individual days over CP (blue curve) with its quiet time reference curve (dark gray curve) brings out the degree of variability in the EIA strength during these disturbed days. In particular we may notice that, starting near 15 LT (arrow 3, sixth panel) on 24 October, the EIA intensity first increased likely as a result of a surge in plasma fountain that is indicated by the equatorial F layer height increase over SL that preceded these changes. In this cause-effect connection we need to allow a delay factor for the EIA foF2 adjustment/response to a rapid change in the zonal electric field (the equatorial fountain surge), which is of the order of 2–4 h as found from model calculations and observational results [see, e.g., *Hanson and Moffet*, 1966; *Abdu et al.*, 1990]. Thus the EIA (foF2) intensification that peaked near 18 LT may be attributed to the preceding height increase at SL and Cachimbo that peaked near 15 LT. We believe these height increases resulted from a PPEF that was associated with the AE activity under the Bz south conditions that prevailed at this time. Similarly the EIA weakening in the post sunset hours starting at 19 LT (that followed the EIA intensification) must be largely the result of a suppressed PRE. On the other hand the EIA presented significant intensification in the post sunset hours of 25 October that was

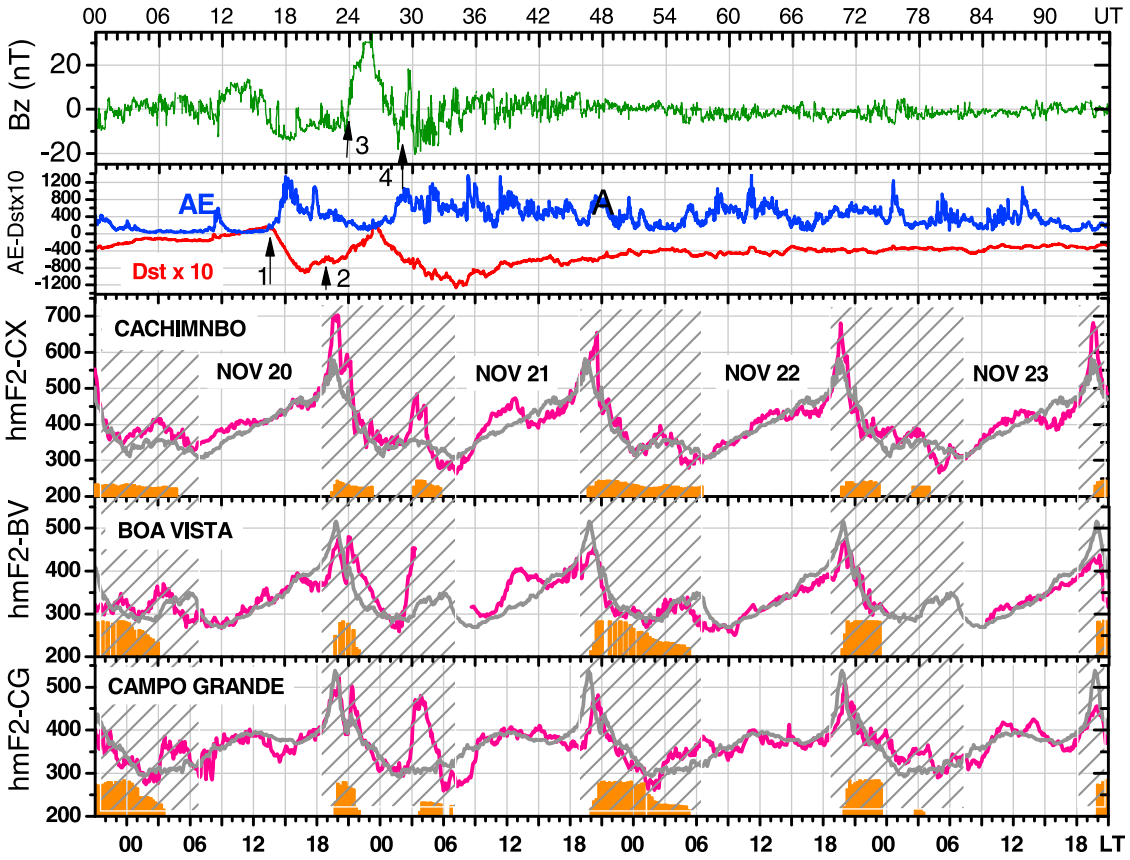

Figure 8a. The 20 November 2002 storm. Plotted are the magnetic indices (the IMF Bz, AE and Dst) (first and second panels) (please note that the Dst is shown multiplied by 10 for plotting convenience), the F layer peak height hmF2 over Cachimbo (third panel), Boa Vista (fourth panel) and Campo Grande (fifth panel). The quiet day reference curve is in gray. The spread F intensity (orange histograms) is plotted in terms of the parameter fop (the top frequency of the spread F trace) given by fop = (y-200)/3. The scale of fop is the same as that shown in Figure 4. Night hours are shown shaded.

the result of an enhanced PRE as can be verified from Figure 5. Further electro-dynamical implications of these EIA responses will be discussed in section 3.3.

2.2. The Moderate Intensity Storm of 20–23 November 2002

[19] In Figure 8a we present the IMF Bz, the auroral electrojet activity AE, and the Dst represented by the SYM-H (first and second panels) for the 20 November 2002 storm. The storm onset near 1330 LT/1630 UT may be noted in the IMF Bz southward turning and the simultaneous rapid intensification of the AE and Dst as indicated by the arrow 1. The hmF2 variations at the three COPEX sites with their respective quiet day reference curves (gray curve) are shown in the third through fifth panels. Also shown is the spread F intensity represented by the parameter fop as was done in Figure 4. The minimum Dst of −120 nT (note that the Dst is multiplied by a factor of 10 for plotting convenience) characterizes this storm as of moderate to intense category. As in the case of the October storm, the intensity of the driving storm energy input for this storm appears to be weaker by approximately a factor of 4 with respect to that of a typical super storm. The F region vertical drift (Vz) for these days obtained by the same method as used for the plots of Figure 5, as well as the parameter $dhmF2_{(CG-BV)}$ are plotted (together with the magnetic indices) in Figure 8b. The interval of the most intense magnetospheric activity during this extended storm, that is, roughly from 09-to-09 LT of 20–21 November, is zoomed-in in Figure 8c to show with better time resolution the responses of the Vz, and the F layer heights at a wide range of plasma frequencies (from 3 MHz to foF2), to changes in storm activity. The southward turning of Bz with the AE and Dst intensifications near 1330 LT/1630 UT (indicated by the arrow 1) and the associated PPEF of eastward polarity produced little/no effect on hmF2 and Vz over Cachimbo. This lack of response is due to a combination of the two factors (mentioned also in section 2.1), namely, the dominating daytime photochemistry of the F layer and the relatively poor penetration efficiency of the PPEF at this local time. Both these factors play steadily decreasing roles approaching sunset, so that a clear Vz decrease (a negative kink) occurred at 18 LT in response to an over-shielding westward electric field associated with the AE recovery (the arrow 2 in Figure 8c). (Apparently the AE increase, which preceded, did not produce a clear signature on the Vz). The negative kink was followed by large increases in the Vz and the F layer height during the PRE.

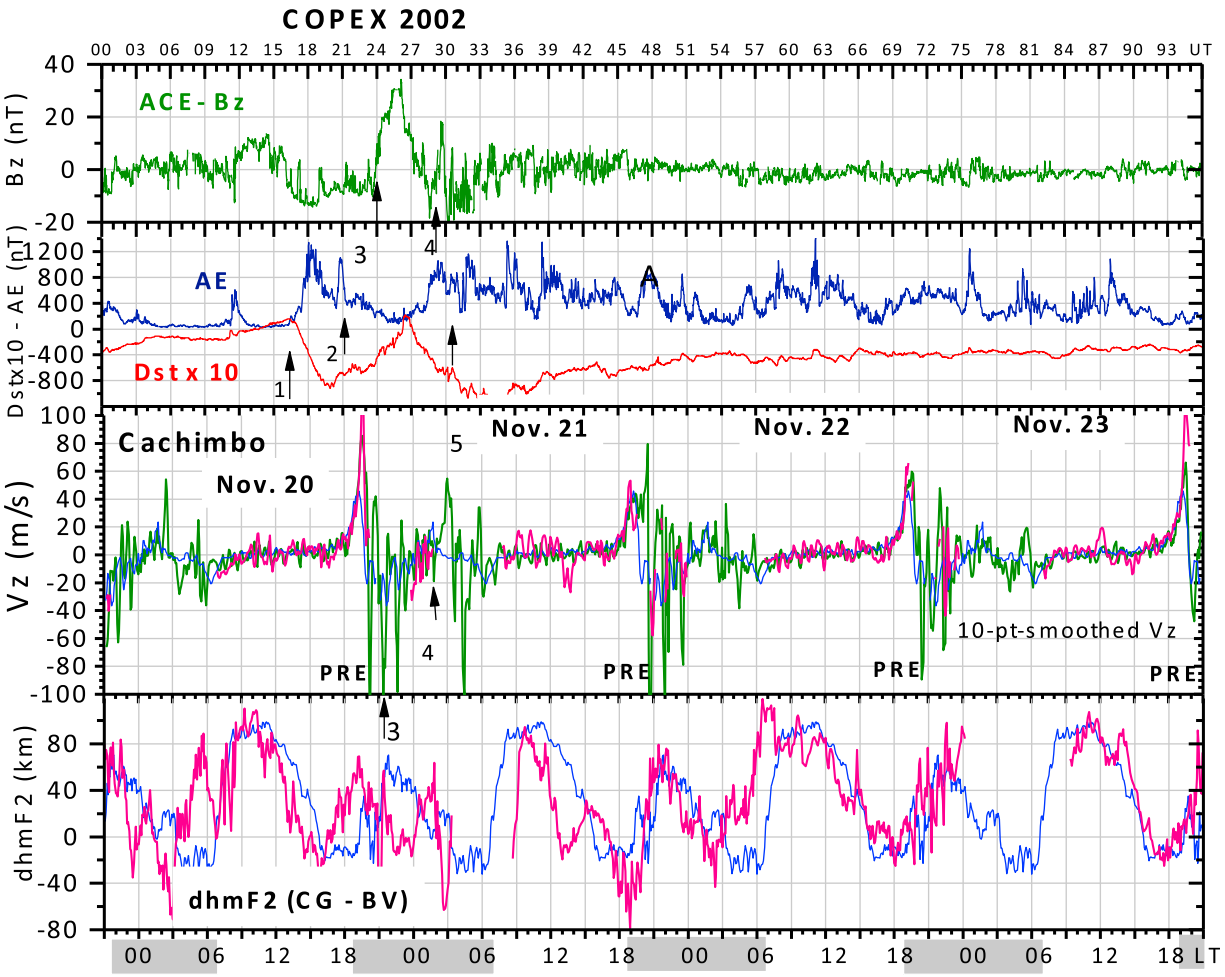

Figure 8b. For the same interval as in Figure 8a are shown: the one-minute magnetic activity indices AE and Sym-H (Dst) (first and second panels), the F region vertical drift in green and pink curves representing the averages of the Vz calculated at 6 and 7 MHz, 10 and 11 MHz, respectively, compared with its reference day curve (blue), the average of four quietest days of the period (third panel), the difference in the hmF2 between the two conjugate sites (dhmF2(CG − BV)) compared with the reference curves (blue) (fourth panel). Night hours are shown shaded at the *x* axis.

This occurred in response to a PPEF of eastward polarity associated with the shallow increases in the AE and Dst activity under the long enduring Bz south condition (Figures 8b and 8c). These AE and Dst increases occur with respect to their otherwise decaying/recovery trends. The peak vertical drift near 1930 LT reached 110 m/s, which corresponded to an eastward electric field of approximately 3 mV/m. This large vertical drift caused prompt development of a plasma bubble as indicated by the 1920 LT ESF onset over Cachimbo (Figure 8c), which is followed by its simultaneous occurrences over the conjugate sites within about 10 min (Figure 8a). The corresponding bubble/plasma depletion rise velocity over the equator can be estimated to be ~400 m/s. A large negative excursion in Vz occurred as the end phase of the PRE, which soon recovered to positive drift. A major downward drift (of >1 h duration) that soon followed (starting near 2050LT) was clearly the results of an over-shielding westward electric field associated with the Bz turning north at this time indicated by the arrow 3 (Figure 8c). As a result of this downdraft and a subsequent negative drift that peaked near 2240 LT the ESF was soon disrupted at all the three sites. The cause of this 2240 LT negative departure in the drift is not clear to us, but it might well be part of a traveling wave disturbance as suggested by the small amplitude oscillations in Vz that continued for a while.

[20] Later during post midnight hours, the Bz started to turn north at 0140 LT (arrow 4, Figure 8c) which caused an over-shielding penetration electric field of eastward polarity, which resulted in vertical drift that reached a peak velocity of 50 m/s. This large vertical drift promptly initiated the development of a plasma bubble event as suggested by the ESF occurrence sequence at the COPEX sites that may be noted in Figure 8a (although there was no data at BV at this time). Interestingly in this case as well, it appears, the ESF

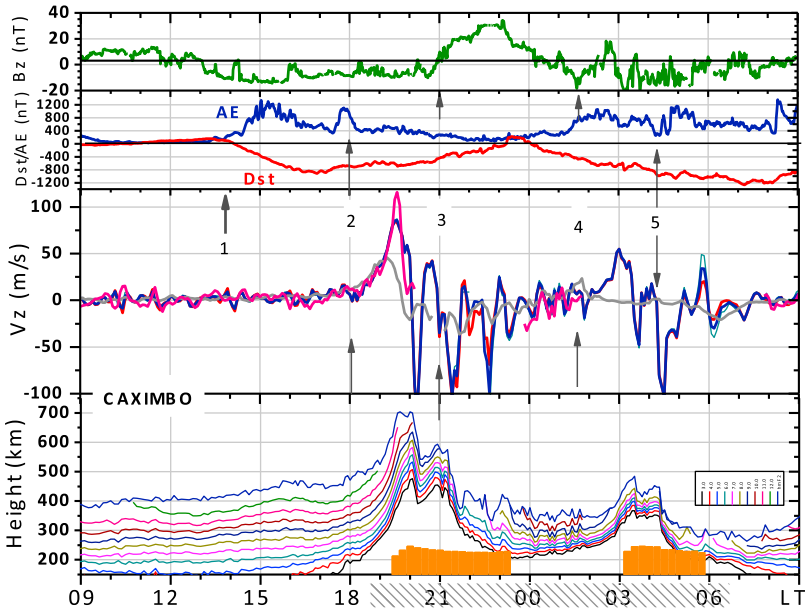

Figure 8c. Part of the Figure 8b zoomed-in for the interval 09 LT to 09 LT on 20–21 November 2002. The Bz, AE and Dst indices are shown in the first and second panels. The vertical drift (Vz) shown in blue and pink corresponds to its mean values calculated from 6 and 7 MHz, and 10 and 11 MHz plasma frequencies, respectively; the quiet day reference curve is shown in gray (third panel). The fourth panel shows the iso lines of true heights at successive plasma frequencies (3 MHz till foF2). Night hours are shaded at the *x* axis.

was disrupted (prior to sunrise, Figure 8c) by a strong plasma downdraft due to an under-shielding westward electric field possibly associated with the Bz south and the prevailing AE activity conditions at this time (arrow 5 in Figure 8c).

[21] Around the noon hours of 21 November (Figure 8a) the F layer height increased significantly, which must be the result of a PPEF (eastward) associated with the AE intensifications under a fluctuating Bz condition even as the Dst was beginning to recover at this time. The eventual Dst recovery that continued into the next two days was marked by episodes of AE intensifications under relatively weaker Bz southward transients. As a result, we may note in Figure 8b, that the PRE vertical drift on these days was higher, around 60 m/s, than its normal quiet time intensity of ~45 m/s. Consequently, plasma bubble development took place on all these evenings as indicated by the spread F occurrences at the conjugate sites in prompt sequence to its occurrence over the equator (Figure 8a). It is interesting that no clear indication of disturbance wind dynamo electric field was identifiable on these days. The short durations (2–3 h) hmF2 decreases in the afternoon of 21, 22, and 23 November (clearly seen over Cachimbo) might look like potential candidates for possible DDEF effects. But the role of over-shielding electric field of westward polarity that must be associated with the AE decreases at these times cannot be ruled out. Additionally, a suppression of the evening PRE vertical drift that is usually expected from a westward DDEF was not observed on any of the evenings during the slow (and long duration) recovery of this moderate intensity storm. It is worth commenting here that the PRE amplitude is large under quiet conditions on 23 November, in Figure 8b, which appears to be the result of a superimposed gravity wave modulation of the F layer heights at higher plasma frequencies at this time.

3. Discussion

[22] Wide ranging aspects of the equatorial ionospheric responses in the Brazilian longitude sector to magnetic storms of moderate intensity that occurred during a period of moderate to high solar flux (the average F10.7 being 165 SFU) were presented above. The storm effects analyzed are in terms of the variations observed in the F layer heights at specific plasma frequencies, the foF2 and hmF2, the evening prereversal vertical drift, spread F development, the inferred trans-equatorial winds (TEW), the EIA intensity, and the zonal plasma drift. Diverse sequential effects were noted in these characteristics depending upon the evolution of storm activity phase and duration. In order to consolidate these results in a coherent way we discuss them further below in terms of a few well-focused cause-effect processes that are currently of outstanding interest in this field. We want to emphasize the point that an in-depth characterization of the plasma bubble/ESF response to disturbance electric fields, especially in regard to the potential role of TEW on storm time ESF (to be discussed below), is made possible because of the conjugate point observations. Among the most outstanding results of this study are those that concern the storm effects on the PRE, ESF, EIA, TEW, and zonal drift, and therefore it is useful to very briefly describe in a general way the connection among them as per our present understanding.

[23] The most important single factor as a precursor condition for the post sunset equatorial spread F (ESF) development is the evening prereversal electric field enhancement (PRE) that causes a rapid uplift of the F layer. The PRE

development is controlled by the longitudinal gradient in the E layer conductivity across the sunset terminator and the thermospheric zonal wind, which turns eastward in the evening [*Rishbeth*, 1971; *Heelis et al.*, 1974]. Plasma instabilities develop by the Rayleigh-Taylor interchange mechanism initiated at the bottom-side gradient region of the rapidly rising F layer. The instability linear growth needs to be initiated by perturbations in background plasma density and polarization electric fields believed to be produced by gravity waves. The nonlinear growth that may follow leads to plasma depleted flux tubes (plasma bubbles) with cascading irregularity structures rapidly rising up to the topside ionosphere marking the development of an ESF event. Both the linear and the nonlinear growth phases are controlled by the field line integrated E- and F-layer Pederson conductivities of the unstable flux tube. The contribution of meridional trans-equatorial winds to instability linear growth is small compared to that of the PRE vertical drift [*Kherani et al.*, 2005]. But such winds can cause asymmetry in the EIA latitudinal structure and increase the field line integrated conductivity, which could retard/suppress the bubble nonlinear growth as was shown from model calculations by *Maruyama* [1988] and verified by recent ionosonde observations [e.g., *Abdu et al.*, 2006a; *Saito and Maruyama*, 2006]. Observations by different techniques show a large degree of day-to-day variability in the intensity and the occurrence of ESF [*Chapagain et al.*, 2009; *Tsunoda*, 2005] which may be caused by the variabilities in (a) the evening prereversal vertical drift, (b) the ambient ionospheric dynamics due to wave disturbances such as from gravity waves needed to seed the instability process, and (c) the thermospheric meridional/trans-equatorial winds that could control the nonlinear growth through field line integrated conductivity, or vertical winds influencing the instability linear growth [*Sekar et al.*, 1994]. As regards the item (a) large variations in the PRE vertical drift can occur from their modulation by planetary waves [*Abdu et al.*, 2006b], and storm time electric fields.

[24] The focused items to be discussed below are (1) the development or suppression of the evening PRE vertical drift and the ESF under storm time electric fields, (2) competing influences of the PRE and TEW in the ESF development, (3) the EIA variability under storm time electric field, and (4) the storm time reversal of disturbance zonal drifts.

3.1. The Development or Suppression of the Evening PRE Vertical Drift and Spread F Due to the Storm Time Electric Fields

[25] As was noted in Figure 5 for the 24 October storm sequence, the response of the vertical drift was mainly in the form of enhanced as well as suppressed intensity of the evening prereversal vertical drift. Correspondingly the spread F/plasma bubble irregularities exhibited enhanced development or did not develop at all. What appears to be a typical case of the PRE partial suppression can be noted on the evening of 24 October when the PRE vertical drift was 20 m/s, which is significantly small as compared to its quiet day mean value of ~50 m/s for this period with F10.7 = 160. The threshold minimum of the PRE vertical drift required to cause plume/bubble type spread F development (that needs to rise to an apex height of 900–1000 km to be observed at Cachoeira Paulista) has been found to be in the range of 30–35 m/s for equinoctial conditions [*Abdu et al.*, 2006a, 2009b] which is consistent with the results from Jicamarca for comparable solar flux values [see *Chapagain et al.*, 2009]. The threshold drift for the bottom-side-only spread F was found to be 22 m/s from the COPEX data by *Abdu et al.* [2009b]. Thus, with the vertical drift of 20 m/s, the non-occurrence of spread F on the evening of 24 October over any of the COPEX sites (Figure 4), or over SL and CP (Figure 7) is consistent with the previous results. It should be pointed out that the threshold velocity just mentioned is a statistical mean value (representing a group of days), and in individual cases it could possibly be significantly modified depending upon the strength of a gravity wave seed perturbation [see, e.g., *Abdu et al.*, 2009c; *Kherani et al.*, 2009], which we will not be discussing here.

[26] An important question concerns the cause of the partial PRE suppression on the evening of 24 October. Since the storm onset was 18 h earlier, with continuing AE activity and the Dst close to the recovery phase, one might expect that a disturbance wind dynamo electric field of westward polarity could have caused the PRE suppression. However, this does not seem to be the case here. The Bz marked a northward turning accompanied by an AE recovery at ~18 LT (arrow 4, Figures 2, 3, 4 and 5) which seems to have produced an over-shielding westward electric field that caused a reduction of the evening eastward electric field thereby contributing to the partial PRE suppression in this case. A recent study [*Abdu et al.*, 2009a] has shown that an over-shielding electric field of westward polarity in the evening sector (during an intense storm activity) can be strong enough to cause a total suppression or even a reversal to downward of the vertical drift. Thus the PRE- and ESF-suppression in this case is likely the result of a penetration electric field originating from an over-shielding process marking the recovery of a substorm episode in the course of a long lasting storm sequence of moderate intensity (see also the discussion in section 3.4). The possible/expected role of a DDEF is not identifiable in this case.

[27] Another case of a PRE partial suppression can be noted on the evening of 26 October (Figure 5). In this case the peak vertical drift was near 35 m/s, which is much smaller than its quiet time peak (50 m/s) but slightly above the statistical minimum threshold (mentioned above) for bubble irregularity development. Spread F did occur over all the three COPEX sites as can be noted in Figure 4. However, the bubble vertical rise velocity appears to be small (of the order of 30 m/s only) as can be inferred from the time delay in the spread F onset at conjugate sites with respect to its equatorial onset. We further note that the spread F occurred also over the equatorial site Sao Luis (Figure 7) with no indication of its occurrence till midnight over CP, which suggested a very small bubble rise velocity consistent with that observed from the conjugate sites. It is not likely that the partial PRE suppression on this evening is caused by an over-shielding westward electric field because the prior AE recovery had been fully completed by 1620 LT (over Cachimbo), ~2.5 h before the PRE partial suppression (Figure 5). A disturbance wind dynamo known to have westward polarity at this local time [*Richmond et al.*, 2003; *Fejer et al.*, 2008] is more likely responsible for the partial suppression of the PRE that resulted in the retarded spread

F/bubble growth on this evening. Thus it is clear from these case studies that the PRE and ESF suppression can occur due to an over-shielding electric field or a disturbance dynamo electric field both of which have westward polarity around the sunset local time. This shows that adequate criteria need to be used for identifying the possible contributions to the causes of post sunset spread F/bubble suppression.

[28] The remaining cases of the PRE responses during the 24 October storm sequence (Figure 5) and all such responses during the four-day interval of the 20 November storm that were analyzed in this study (Figures 8b and 8c) are marked by enhanced vertical drift as compared to the quiet time drifts. A clear case of such enhanced vertical drift of the PRE occurred on the evening of 25 October (arrow 6 at 18 LT in Figure 5). The peak vertical drift was 80 m/s, large indeed as compared to the quiet time value of ~50 m/s. This large vertical drift was responsible for the spread F/bubble irregularity development over the COPEX sites as well as over SL and CP (Figures 4 and 7). It is interesting to note further that the SF was soon disrupted at all the sites (not clear at CP due to missing data) under the downward plasma drift that followed the upward drift. The cause of the large upward drift appears to be a prompt penetration electric field of eastward polarity associated with the rapid increase in AE (by ~500 nT), with the Bz increasing southward near 18 LT (arrow 6 in Figure 2). The AE recovery that occurred near 21 LT with the Bz turning north appears to be responsible for the downward plasma drift that resulted in the ESF disruption (near 23 LT on 25 October, Figure 4). A similar explanation based on the effect of a PPEF/PEF may apply also for the major vertical drift enhancements observed during the 20 November storm sequence, plotted in Figures 8a, 8b and 8c. In this latter case even though the end of the storm was on the fringe of a period affected by a planetary wave activity that modulated the PRE vertical drift as discussed by *Abdu et al.* [2006b], a rather clear signature of the storm associated PPEF can be identified. The large increase in the vertical drift (~110 m/s) during the PRE on the evening of 20 November (Figures 8b and 8c), induced by a PPEF, produced prompt spread F bubble development over the COPEX sites (Figures 8a and 8c) soon to be disrupted by large downward drift at 2130 LT (Figure 8c), indicated also by a rapid layer fall (Figure 8a). The relatively longer duration down-drift that set in when Bz turned north at 21 LT (arrow 3, Figure 8c) and the other short duration down-drift at 2240 LT are believed to be the main reason for the ESF disruption that followed. Thus we have here a clear sequence of an under-shielding PPEF of eastward polarity generating an ESF event, followed by an over-shielding westward polarity electric field that contributed to the disruption of the ESF (as on the evening of 25 October). We commented before (based on model and observational results) that the penetration electric field reverses its polarity near/after midnight. The consequence of such polarity reversal on the ESF development may be noted as follows. In the post midnight hours of 20–21 November an over-shielding eastward electric field associated with the Bz beginning to turn north (indicated by the arrow 4 in Figures 8a, 8b and 8c) caused large upward vertical drift (50 m/s) that resulted in ESF bubble development but to be soon disrupted (Figure 8c) by an under-shielding westward electric field (downward drift) associated with an AE intensification under Bz south condition (arrow 5, Figure 8c). Thus while an ESF development and disruption sequence in the post sunset hours follows under-shielding and over-shielding electric fields, respectively, in the post midnight hours such ESF sequence follows over-shielding and under-shielding electric fields, respectively.

[29] Although the Dst recovery started in the morning of 21 November the fluctuating AE activity in the presence of weak Bz southward excursions seems to have produced PPEF, which dominated the F layer height fluctuations during the following three days. Interestingly we do not observe (in Figure 8a) any clear and significant height variation that can be uniquely attributed to disturbance wind dynamo during these storm sequences.

3.2. Relative Influences of the PRE and TEW in the SF Development

[30] The role of the TEW in suppressing the ESF generation during quiet time has been reasonably well demonstrated from ionosonde observations [e. g., *Abdu et al.*, 2006a, 2009b; *Saito and Maruyama*, 2006]. Under this premise we will examine the effect of the TEW observed during these moderate intensity storms. In Figure 5 we may notice that on three evenings (around 18 LT) following the start of the 24 October storm the TEW, as indicated by the parameter $dhmF2_{(CG-BV)}$, is more intense southward than on the day before the storm development (23 October). In the case of the 20 November storm the TEW was higher than normal (also southward) on the evening of 21 November only (Figure 8b). Possible effect of such enhanced TEW on the post sunset spread F development can be examined as follows.

[31] The TEW can influence the post sunset spread F development through its ability to cause asymmetry in the EIA and to enhance the field line integrated conductivity that can reduce the nonlinear growth of an instability process and thereby cause the suppression of the bubble development [*Maruyama*, 1988; *Abdu et al.*, 2006a; see also *Basu et al.*, 2009]. This possibility cannot be verified for the conditions on the evening of 24 October (in Figure 5) since the PRE was not sufficient to cause the needed linear growth rate in the first place. This result shows that the role of TEW to suppress the bubble development can be determined only when the PRE is of sufficient intensity, being above a threshold value (~35 m/s), for positive instability linear growth rate.

[32] The competing influences of the PRE and TEW on spread F/bubble development can be examined perhaps in a more critical way for the conditions prevailing on 25 October evening. On this evening the PRE vertical drift (enhanced by a PPEF) peaked at 80 m/s (Figure 5), and well-grown bubble development took place as evidenced by the spread F occurrence at all the COPEX sites (Figure 4) as well as over SL and CP (Figure 7). The TEW increased southward on this evening more than it did on the previous evening. Although the amplitude of the enhanced wind was estimated to be of the order of 50 m/s, it was not sufficient to suppress the nonlinear growth of the R-T instability initiated by the large PRE vertical drift of 80 m/s, as evidenced by the occurrence of well-developed bubbles. During the 20 November storm sequence a small enhancement of TEW was observed on the evening of 21 November (Figure 8b), but, because of a

relatively large PRE vertical drift (55 m/s), the spread F bubble development was apparently not affected by the TEW. We need to point out here that the amplitude of the gravity waves precursor for the R-T instability initiation (that is, the seeding perturbation) can control the threshold limit of the vertical drift required for a given intensity of the bubble development [*Abdu et al.*, 2009c; *Kherani et al.*, 2009]. From these examples, therefore, we are able to affirm that, although there could be some uncertainty arising from gravity wave contribution in the instability seeding process, our simplified and qualitative considerations appear to suggest that the potential role of a TEW for suppressing the nonlinear growth for bubble formation can be overcome by enhanced intensity of the PRE vertical drift during moderate intensity storms. This finding is made possible only by the conjugate point observations. Only a numerical simulation of the interconnected processes can give us an idea on the quantitative limits of the competing factors (that is, the PRE versus TEW), in the presence of given gravity wave triggers, to be effective in the spread F/bubble development.

3.3. The EIA Under Storm Time Electric Field

[33] The equatorial ionization anomaly (EIA) can suffer significant modification under storm time electric fields. During intense/super storms, the strong prompt penetration electric field having eastward polarity during the daytime and evening hours can cause the EIA crests to expand to midlatitudes. Large latitudinal expansion of the EIA, due to PPEF in the evening hours, as observed in the ionospheric TEC data in the Brazilian-Atlantic longitude sector during the March 1989 super storm was reported by *Abdu* [1997]. Large increase in the daytime TEC and EIA expansion to mid latitude (under strong eastward PPEF) were observed in the GPS TEC data in the daytime Pacific sector by *Tsurutani et al.* [2004], *Mannucci et al.* [2005], *Lin et al.* [2005] and *Zhao et al.* [2005], during the severe storm events of November 2001 and October 2003. On the other hand the disturbance wind dynamo electric field (DDEF) that can dominate the later hours of a storm sequence has westward polarity during daytime and evening hours, in the latter case the PRE vertical drift being suppressed. Thus the EIA can suffer suppression during daytime and post sunset hours due to DDEF.

[34] During storms of moderate intensity such as in the present case the EIA latitudinal expansion may not be significant. But enhancement/suppression of the EIA intensity does occur depending upon whether the storm time electric field is under-shielding or over shielding type, or originating from disturbance wind dynamo. Daytime EIA suppression due to DDEF was reported by *Sreeja et al.* [2009] during a moderate storm of January 2005. Such daytime EIA suppression generally occurs in association with the equatorial electrojet (EEJ) attenuation, as both are controlled by the same equatorial zonal electric field [see, e.g., *Sastri*, 1988; *Le Huy and Amory-Mazaudier*, 2005; *Zaka et al.*, 2009; *Rastogi and Klobuchar*, 1990]. We may examine the EIA response features with the help of the foF2, hmF2 and F layer height variations over the EIA trough (crest) location Sao Luis (Cachoeira Paulista) plotted in Figure 7. Starting at 15 LT of 24 October (arrow 3) we note EIA foF2 enhancement over CP (sixth panel) that was caused most likely by an under-shielding PPEF of eastward polarity associated with the AE intensifications that occurred near this time and during the preceding hours. As mentioned earlier a delay of 2–3 h is clearly evident in the EIA foF2 response with respect to the height increase over the equatorial site (SL) (fifth panel). We notice further that starting at sunset the EIA is weakened because of a reduced fountain due to a suppressed PRE vertical drift (arrow 4, Figure 5). The F layer height over SL was also severely reduced as compared to the previous evening (Figure 7). This weakening was in response to a northward turning of the Bz accompanied by AE recovery that occurred at this time (see also Figure 2). In addition to the ESF suppression the EIA was weakened. The weakened EIA prevailed till ~03 LT of 25 October. An AE partial recovery associated with a Bz northward transition occurred at ~23 LT (of 24 Oct) whose effect on the hmF2 and foF2, if any, is difficult to assess (especially because the penetration electric field is known to reverse the polarity near this local time [see *Fejer et al.*, 2008]. The next major AE increase (also associated with Bz southward excursion) was that starting at ~07 LT on 25 Oct and that lasted for about 5 h, and the resulting PPEF appears to be responsible for maintaining the foF2 at its reference mean level till about midday, perhaps opposing the effect of a westward DDEF that should have (if present) decreased the foF2 at these hours. The hmF2 and foF2 remained above normal in the following hours with relatively weaker AE activity. Then near sunset the PRE vertical drift (~80 m/s) was significantly higher than normal due to an under-shielding electric field associated with an AE intensification that occurred right at this time (as explained before, arrow 6, Figure 5). This enhanced PRE was responsible for the subsequent EIA intensification that prevailed till sunrise on 26 October. We may recall in this context the ESF development that also occurred as a result of the large PRE (section 3.1). Though the data was discontinuous over CP during 1930–2300LT, the delay factor in the EIA foF2 response to the equatorial height increase can be noticed in Figure 7, that is, the EIA foF2 increase appears delayed and persists longer with respect to the equatorial height increase. It appears that while the ESF develops promptly in response to an enhanced PRE (as mentioned in section 3.1) the associated EIA development could attain full strength only after some additional time delay. The PPEF associated with the AE activity again increased with consequent effects on the F layer heights during the day hours of 26 October. Thus we note that during this moderate storm activity sequences the effect of PPEF of eastward polarity dominated the day hours making difficult the identification of any DD electric field effect, if present. As regards the EIA we note that its post sunset development can be weakened due to an over-shielding electric field of westward polarity in the evening hours (as on 24 October) whereas it can be enhanced due to an under-shielding electric field of eastward polarity also in the evening-night hours (as on 25 October). Also, such responses have a time delay of 2–4 h with respect to their driving electric fields. The present data set is not sufficient, however, to provide us information on any latitudinal contraction/expansion of the EIA under these electric fields. Cases of interplay of under-shielding and over-shielding electric fields and their roles in simultaneous EIA development/suppression in the Asian/Brazilian longitude sectors during

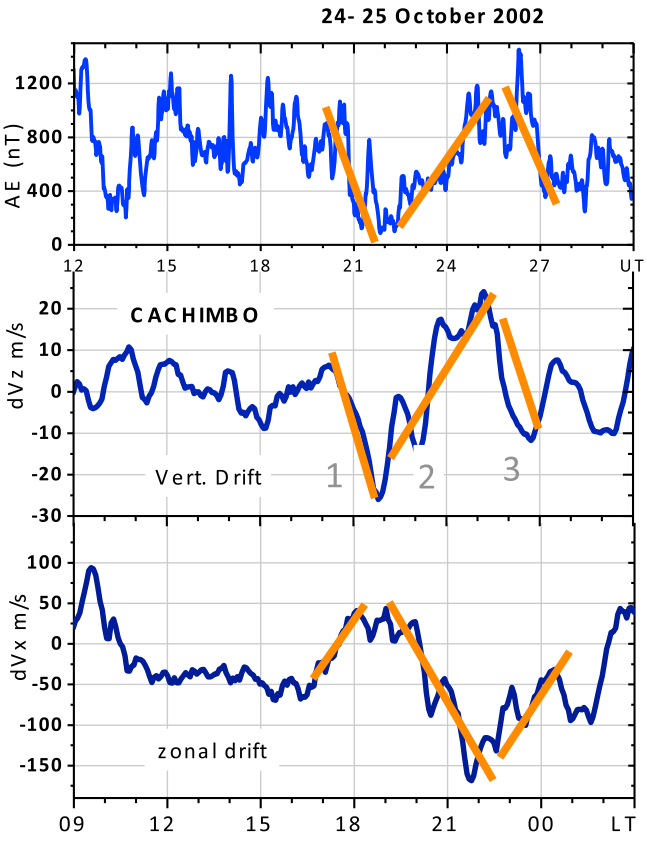

Figure 9. (top) The AE index, (middle) the vertical drift difference dVz and (bottom) zonal drift difference during 24–25 October 2002. The drift differences, dVz and dVx were obtained by subtracting the quiet day drift from the individual day drift.

the October 2003 super-storm events have been discussed by *Abdu et al.* [2007].

3.4. Storm Time Disturbance Zonal Drifts

[35] The zonal plasma drifts over the COPEX sites plotted in Figure 6 for 24–25 October show significant differences from their quiet time values, the disturbance drifts being more westward in the evening and post sunset hours. The difference appears to be better defined over the equatorial site Cachimbo than over the other two sites. The zonal plasma drift is generally considered to be a tracer of the background thermospheric zonal wind, especially during nighttime when the reduced E layer conductivity is sufficiently small to maintain a good degree of electrical decoupling between the E and F layers. Therefore a westward increase of the zonal drift such as that found in the present result could be indicative of the presence of a westward disturbance thermospheric wind. Previous observations, and more recently CHAMP satellite observation during intense/severe storms have shown significant enhancement in westward thermospheric winds over mid- to equatorial-latitudes [*Sutton et al.*, 2005]. Observations of zonal plasma bubble irregularity drift using optical all-sky imager and GPS scintillation receivers, also during the COPEX campaign, showed reduced eastward velocity under disturbed (higher ΣKp) conditions which was attributed to an increase of westward thermospheric wind [*Sobral et al.*, 2009]. The westward wind increase is expected from Coriolis effect on the equatorward propagating winds originating from auroral heating process under storm energy input. Such winds are known to be responsible for the disturbance dynamo electric field [*Blanc and Richmond*, 1980; *Richmond et al.*, 2003] that has westward polarity during the daytime and evening hours. Over the equatorial region the PRE vertical drift can be suppressed by this electric field as well as by the direct interaction of a westward wind with the normally eastward thermospheric wind basically responsible for the quiet time PRE development. The vertical drift around the partial PRE suppression on 24 October (in Figure 5), however, is likely less influenced by these factors as was noted in section 3.1 and in the light of the discussion below.

[36] The nature of the vertical drift variation surrounding this partial PRE suppression can be understood from the plots in Figure 9 that show the vertical and zonal drift differences and the simultaneous AE variations during a 24-h period 09–09 LT of 24–25 October. The drift differences were obtained by subtracting the quiet/reference day drifts from the disturbed day drifts. We may notice that from ∼17 LT till ∼00 LT the disturbance vertical drift follows closely the average trend in the AE variation; the trends are indicated by the straight lines drawn on the plots. (The lack of such correlated trends between the two parameters, outside of this local time interval, has to do with the factors mentioned before: the daytime photo-chemistry and the local time of reduced efficiency of the penetration electric field). The negative deviation in the vertical drift (dVz) near 18 LT (identified as '1') occurs right at the time of an AE recovery, thereby suggesting (as noted before) that an over-shielding electric field of westward polarity must be responsible for the partial suppression of the PRE that occurred at this time (see also Figure 5). Subsequently, from ∼19 to ∼23 LT, the AE activity intensified with Bz turning south (Figure 2), and the associated under-shielding eastward electric field was responsible for the dVz to grow positive (indicated by '2'). The AE partial recovery with superimposed fluctuations that followed (related to a transient Bz north condition) produced a dVz negative deviation (indicated as '3') as expected from an over-shielding westward electric field. Thus we notice a control by penetration electric fields in this vertical drift episode. At the same time the simultaneous variations in the zonal drift deviation, dVx, appear very interesting. There is a general trend of anti-correlation between the variations in the AE and in dVx starting from near midday till midnight. The region identified as 1, 2, and 3 is especially interesting since we note that a connection between the disturbance vertical drift and zonal drift is evident here, and such connection is driven by AE intensification and recovery phases. In other words, an under-shielding eastward electric field produces an upward perturbation in vertical drift that is accompanied by a westward perturbation in zonal drift, while an over-shielding westward electric field produces a downward drift perturbation that is accompanied by an eastward perturbation in the drift. Such a connection between the vertical and zonal drifts can exist only if the penetrating zonal electric field induces a vertical/field line perpendicular electric field by Hall conduction and by vertical current flow arising from divergence of horizontal currents as explained for the first

time by *Abdu et al.* [1998] [see also *Abdu et al.*, 2003]. Further to the previous studies (that covered night hours only) the present result shows for the first time the Hall conduction operating during the hours leading to the PRE vertical drift as well. Using a general expression for the F region vertical electric field based on field line integrated parameters as derived by *Haerendel et al.* [1992], and considering the transient nature of the penetration zonal electric field, and therefore neglecting any contribution from zonal wind and vertical currents to the disturbance vertical electric field, as explained in *Abdu et al.* [2003], we have the following relationship between the disturbance zonal electric field $\Delta E\varphi$ and vertical electric field ΔE_L:

$$\Delta E_L = (\sum_H / \sum_P) \Delta E\varphi$$

Here $\sum_H$ and $\sum_P$ are the field line integrated Hall and Pederson conductivities. This equation clearly shows that for a given conductivity ratio an increase in the eastward electric field (upward vertical drift) will result in an increase of upward electric field (westward plasma drift). Similarly an increase in westward electric field would result in a downward increase in the electric field/eastward plasma drift. This situation requires a significant degree of E layer ionization enhancement. For the intense storm on 19 October 1998 *Fejer and Emmert* [2003] observed a near midday episode of westward plasma drift in association with the vertical drift. They attributed the westward drift as caused by Hall conduction effect induced by the primary eastward PPEF responsible for the associated vertical drift. For the Hall conduction effect to be observed during the evening-night hours as in the present case, the required conductivity ratio could be produced, we believe, by storm associated energetic particle precipitation. Such a source of ionization is known to be present in the Brazilian/South Atlantic Anomaly region (SAMA) as per previous studies [see, e.g., *Abdu et al.*, 1998, 2005, and references therein]. Ionosonde observations in this region have established that significant enhancement in E layer plasma density can occur due to precipitation of energetic particles during magnetic storms [*Batista and Abdu*, 1977]. The energy distribution of the precipitating particles should be such that the ionization enhancement occurs predominantly in the height region of high Hall mobility (near 120 km) in preference to higher heights where Pederson mobility dominates. Such a situation is conceivable in view of the fact that the magnetospheric electric field could exercise significant control on the azimuthal drift rate and precipitation of inner belt electrons in the SAMA region. The degree of such control is dependent on the energy of the precipitating electrons in the spectral range that affect the height region of our interest (>100 km). The electric field influence increases with decrease in energy (and therefore the drift rate) of the precipitating electrons. In this way the electron precipitation dominating the height region of Hall conductance will be displaced in longitude with respect to that of the Pederson conductance, since the energy of the precipitating electrons in the former case (10–15 KeV) is significantly higher than that in the latter case (2–3 KeV). (Further elaboration on this point will be presented elsewhere). It is beyond the scope of this paper to determine the precise nature of the E region ionization enhancement required to account quantitatively for the observed vertical electric field induced by the primary penetration zonal electric field. The main point of interest here is the following. The storm time thermospheric zonal wind in the mid to equatorial latitudes has been known to be directed westward (based on observations and model studies) and in the post sunset hours it can drive westward plasma drift. However, there are frequent cases of westward plasma drift in the post sunset equatorial ionosphere that are unrelated to such processes but are driven by prompt penetration electric fields [see also *Abdu et al.*, 1998, 2003]. Such disturbance zonal drift can be westward or eastward. In our present results (Figure 9) it appears to be dominantly westward, however.

4. Conclusions

[37] We have presented the results of a study on the equatorial ionospheric response to two magnetic storms of moderate intensity that occurred during the COPEX 2002 Brazilian campaign period. These results have provided new insight into the storm time responses of the low latitude ionosphere with respect to the electrodynamical processes controlling its diverse phenomenology. Specifically, we have addressed disturbance effects on plasma vertical and zonal drifts, the conditions for the development or the suppression of the prereversal vertical drift, plasma bubble generation, and the EIA under different storm phases. The main conclusions of this study may be summarized as follows:

[38] 1. The equatorial F layer heights and vertical plasma drift responses to prompt penetration electric fields, as observed by Digisondes during moderate intensity long lasting storms, exhibit local time dependent features that are in good agreement with the available satellite observations and model results.

[39] 2. In the course of long lasting storms of moderate intensity the auroral electrojet intensification accompanied by Bz south (even if marginally south) condition can cause prompt penetration (under-shielding) electric field of eastward polarity in the sunset sector that may enhance the PRE vertical drift leading to post sunset ESF/bubble development and EIA intensification.

[40] 3. Partial suppressions of the evening prereversal electric field and total suppression of the post sunset spread F/bubbles generation can result from a westward over-shielding electric field during a sub storm recovery occurring near sunset. An ESF activity in progress can be disrupted by an over-shielding (under-shielding) electric field during generally pre midnight (post midnight) hours.

[41] 4. The asymmetry in the conjugate point F layer heights and vertical drifts is attributed to the trans-equatorial winds. They did not, however, suppress the development of spread F, in our study, because of the countering effects of the PRE that caused strong vertical drift.

[42] 5. The presence of a disturbance wind dynamo was not, in general, conspicuous during almost the entire intervals of both of these moderate intensity long duration storms.

[43] 6. Post sunset equatorial ionization anomaly development can be enhanced or suppressed by an under-shielding or an over-shielding penetration electric field, respectively,

when they occur at these hours. Such responses are delayed by 2–4 h with respect to their driving electric fields.

[44] 7. The present results also lead us to conclude that in the longitude sector of this study the storm time zonal plasma drifts are often driven by a vertical Hall electric field that is induced by the primary penetration zonal electric field in the presence of storm time enhanced E layer conductivity. The disturbance in zonal drift can be westward or eastward depending upon the polarity of the PPEF.

[45] Further elucidation of the different aspects discussed above can be achieved from conjugate point and multi-instrument observations using distributed observatories such as GIRO [*Reinisch and Galkin*, 2011] and the one being developed within the LISN project [*Valladares and Doherty*, 2009], and the EMBRACE (Space weather project) by INPE covering the South American low latitude region, as well as from observations by CNOFS and other satellites of opportunity.

[46] **Acknowledgments.** MAA acknowledge support from CNPq through grants 300883/2008-0. BWR was in part supported by AF grant FA8718-06-C-0072. Logistical support for the operations of the instruments at the conjugate sites (Campo Grande, Cachimbo, and Boa Vista) was provided by the Brazilian Aeronautic Ministry's Instituto Tecnologico de Aeronautica (CTA), which is thankfully acknowledged.

[47] Robert Lysak thanks the reviewers for their assistance in evaluating this paper.

References

Abdu, M. A. (1997), Major phenomena of the equatorial ionosphere-thermosphere system under disturbed conditions, *J. Atmos. Sol. Terr. Phys.*, *59*, 1505–1519, doi:10.1016/S1364-6826(96)00152-6.

Abdu, M. A., G. O. Walker, B. M. Reddy, J. H. A. Sobral, B. G. Fejer, T. Kikuchi, N. B. Trivedi, and E. P. Szuszcewicz (1990), Electric field versus neutral wind control of the equatorial anomaly under quiet and disturbed conditions: A global perspective, *Ann. Geophys.*, *8*(6), 419–430.

Abdu, M. A., P. T. Jayachandran, J. W. MacDougall, and J. H. A. Sobral (1998), Equatorial F region zonal plasma irregularity drifts under magnetospheric disturbances, *Geophys. Res. Lett.*, *25*, 4137–4140, doi:10.1029/1998GL900117.

Abdu, M. A., I. S. Batista, H. Takahashi, J. MacDougall, J. H. Sobral, A. F. Medeiros, and N. B. Trivedi (2003), Magnetospheric disturbance induced equatorial plasma bubble development and dynamics: A case study in Brazilian sector, *J. Geophys. Res.*, *108*(A12), 1449, doi:10.1029/2002JA009721.

Abdu, M. A., I. S. Batista, A. J. Carrasco, and C. G. M. Brum (2005), South Atlantic magnetic anomaly ionization: A review and a new focus on electrodynamic effects in the equatorial ionosphere, *J. Atmos. Sol. Terr. Phys.*, *67*, 1643–1657, doi:10.1016/j.jastp.2005.01.014.

Abdu, M. A., K. N. Iyer, R. T. de Medeiros, I. S. Batista, and J. H. A. Sobral (2006a), Thermospheric meridional wind control of equatorial spread F and evening prereversal electric field, *Geophys. Res. Lett.*, *33*, L07106, doi:10.1029/2005GL024835.

Abdu, M. A., P. P. Batista, I. S. Batista, C. G. M. Brum, A. J. Carrasco, and B. W. Reinisch (2006b), Planetary wave oscillations in mesospheric winds, equatorial evening prereversal electric field and spread F, *Geophys. Res. Lett.*, *33*, L07107, doi:10.1029/2005GL024837.

Abdu, M. A., T. Maruyama, I. S. Batista, S. Saito, and M. Nakamura (2007), Ionospheric responses to the October 2003 superstorm: Longitude/local time effects over equatorial low and middle latitudes, *J. Geophys. Res.*, *112*, A10306, doi:10.1029/2006JA012228.

Abdu, M. A., et al. (2008), Abnormal evening vertical plasma drift and effects on ESF and EIA over Brazil-South Atlantic sector during the 30 October 2003 super storm, *J. Geophys. Res.*, *113*, A07313, doi:10.1029/2007JA012844.

Abdu, M. A., E. A. Kherani, I. S. Batista, and J. H. A. Sobral (2009a), Equatorial evening prereversal vertical drift and spread F suppression by disturbance penetration electric fields, *Geophys. Res. Lett.*, *36*, L19103, doi:10.1029/2009GL039919.

Abdu, M. A., I. S. Batista, B. W. Reinisch, J. R. de Souza, J. H. A. Sobral, T. R. Pedersen, A. F. Medeiros, N. J. Schuch, E. R. de Paula, and K. M. Groves (2009b), Conjugate Point Equatorial Experiment (COPEX) campaign in Brazil: Electrodynamics highlights on spread F development conditions and day-to-day variability, *J. Geophys. Res.*, *114*, A04308, doi:10.1029/2008JA013749.

Abdu, M. A., E. Alam Kherani, I. S. Batista, E. R. de Paula, D. C. Fritts, and J. H. A. Sobral (2009c), Gravity wave initiation of equatorial spread F/plasma bubble irregularities based on observational data from the SpreadFEx campaign, *Ann. Geophys.*, *27*, 2607–2622, doi:10.5194/angeo-27-2607-2009.

Akasofu, S., and S. Chapman (1972), *Solar-Terrestrial Physics*, Oxford Univ. Press, London.

Balan, N., et al. (2011), A statistical study of the response of the dayside equatorial F_2 layer to the main phase of intense geomagnetic storms as an indicator of penetration electric field, *J. Geophys. Res.*, *116*, A03323, doi:10.1029/2010JA016001.

Basu, S., Su. Basu, K. M. Groves, H.-C. Yeh, S.-Y. Su, F. J. Rich, P. J. Sultan, and M. J. Keskinen (2001), Response of the equatorial ionosphere in the South Atlantic region to the great magnetic storm of July 15, 2000, *Geophys. Res. Lett.*, *28*, 3577–3580, doi:10.1029/2001GL013259.

Basu, S., Su. Basu, F. J. Rich, K. M. Groves, E. MacKenzie, C. Coker, Y. Sahai, P. R. Fagundes, and F. Becker-Guedes (2007), Response of the equatorial ionosphere at dusk to penetration electric fields during intense magnetic storms, *J. Geophys. Res.*, *112*, A08308, doi:10.1029/2006JA012192.

Basu, Su., S. Basu, J. Huba, J. Krall, S. E. McDonald, J. J. Makela, E. S. Miller, S. Ray, and K. Groves (2009), Day-to-day variability of the equatorial ionization anomaly and scintillations at dusk observed by GUVI and modeling by SAMI3, *J. Geophys. Res.*, *114*, A04302, doi:10.1029/2008JA013899.

Batista, I. S., and M. A. Abdu (1977), Magnetic storm associated delayed sporadic E layer enhancement in the Brazilian Geomagnetic Anomaly, *J. Geophys. Res.*, *82*, 4777–4783, doi:10.1029/JA082i029p04777.

Batista, I. S., E. R. de Paula, M. A. Abdu, and N. B. Trivedi (1991), Ionospheric effects of the 13 March 1989 magnetic storm at low latitudes, *J. Geophys. Res.*, *96*, 13,943–13,952, doi:10.1029/91JA01263.

Batista, I. S., M. A. Abdu, J. R. Souza, F. Bertoni, M. T. Matsuoka, P. O. Camargo, and G. J. Bailey (2006), Unusual early morning development of the equatorial anomaly in the Brazilian sector during the Halloween magnetic storm, *J. Geophys. Res.*, *111*, A05307, doi:10.1029/2005JA011428.

Batista, I. S., M. A. Abdu, A. J. Carrasco, B. W. Reinisch, E. R. de Paula, N. J. Schuch, and F. Bertoni (2008), Equatorial spread F and sporadic E-layer connections during the Brazilian Conjugate Point Equatorial Experiment (COPEX), *J. Atmos. Sol. Terr. Phys.*, *70*, 1133–1143, doi:10.1016/j.jastp.2008.01.007.

Bittencourt, J. A., and M. A. Abdu (1981), A theoretical comparison between apparent and real vertical ionization drift velocities in the equatorial F region, *J. Geophys. Res.*, *86*, 2451–2454, doi:10.1029/JA086iA04p02451.

Blanc, M., and A. D. Richmond (1980), The ionospheric disturbance dynamo, *J. Geophys. Res.*, *85*, 1669–1686, doi:10.1029/JA085iA04p01669.

Chapagain, N. P., B. G. Fejer, and J. L. Chau (2009), Climatology of post-sunset equatorial spread *F* over Jicamarca, *J. Geophys. Res.*, *114*, A07307, doi:10.1029/2008JA013911.

Coley, W. R., R. A. Heelis, and N. W. Spencer (1994), Comparison of low-latitude ion and neutral zonal drifts using DE 2 data, *J. Geophys. Res.*, *99*(A1), 341–348, doi:10.1029/93JA02205.

Fejer, B. G. (1986), Equatorial ionospheric electric fields associated with magnetospheric disturbances, in *Solar Wind Magnetosphere Coupling*, edited by Y. Kamide and J. A. Slavin, pp. 519–545, Terra Sci., Tokyo, doi:10.1007/978-94-009-4722-1_37.

Fejer, B. G., and J. T. Emmert (2003), Low-latitude ionospheric disturbance electric field effects during the recovery phase of the 19–21 October 1998 magnetic storm, *J. Geophys. Res.*, *108*(A12), 1454, doi:10.1029/2003JA010190.

Fejer, B. G., R. W. Spiro, R. A. Wolf, and J. C. Foster (1990), Latitudinal variation of perturbation electric fields during magnetically disturbed periods: 1986 SUNDIAL observations and model results, *Ann. Geophys.*, *8*, 441–454.

Fejer, B. G., E. R. de Paula, S. A. Gonzalez, and R. F. Woodman (1991), Average vertical and zonal F region plasma drifts over Jicamarca, *J. Geophys. Res.*, *96*, 13,901–13,906, doi:10.1029/91JA01171.

Fejer, B. G., J. W. Jensen, and S.-Y. Su (2008), Seasonal and longitudinal dependence of equatorial disturbance vertical plasma drifts, *Geophys. Res. Lett.*, *35*, L20106, doi:10.1029/2008GL035584.

Fuller-Rowell, T. J., G. H. Millward, A. D. Richmond, and M. V. Codrescu (2002), Storm-time changes in the upper atmosphere at low latitudes, *J. Atmos. Sol. Terr. Phys.*, *64*, 1383–1391, doi:10.1016/S1364-6826(02)00101-3.

Gonzalez, W. D., J. A. Joselyn, Y. Kamide, H. W. Kroehl, G. Rostoker, B. T. Tsurutani, and V. M. Vasyliunas (1994), What is a geomagnetic storm?, *J. Geophys. Res.*, *99*(A4), 5771–5792, doi:10.1029/93JA02867.

Greenspan, M. E., C. E. Rasmussen, W. J. Burke, and M. A. Abdu (1991), Equatorial density depletions observed at 840 km during the great storm of March 1989, *J. Geophys. Res.*, *96*, 13,931–13,942, doi:10.1029/91JA01264.

Haerendel, G., J. V. Eccles, and S. Cakir (1992), Theory of modeling the equatorial evening ionosphere and the origin of the shear in the horizontal plasma flow, *J. Geophys. Res.*, *97*, 1209–1223, doi:10.1029/91JA02226.

Hanson, W. B., and R. J. Moffet (1966), Ionization transport in the equatorial *F* region, *J. Geophys. Res.*, *71*, 5559–5572, doi:10.1029/JZ071i023p05559.

Heelis, R. A., P. C. Kendall, R. J. Moffet, D. W. Windle, and H. Rishbeth (1974), Electrical coupling of the *E*- and *F*-regions and its effect on the *F*-region drifts and winds, *Planet. Space Sci.*, *22*, 743–756, doi:10.1016/0032-0633(74)90144-5.

Horvath, I., and B. C. Lovell (2010), Large scale traveling ionospheric disturbances impacting equatorial ionization anomaly development in the local morning hours of the Halloween Superstorms on 29–30 October 2003, *J. Geophys. Res.*, *115*, A04302, doi:10.1029/2009JA014922.

Huang, C.-M., A. D. Richmond, and M.-Q. Chen (2005), Theoretical effects of geomagnetic activity on low-latitude ionospheric electric fields, *J. Geophys. Res.*, *110*, A05312, doi:10.1029/2004JA010994.

Huang, C.-S., J. C. Foster, and M. C. Kelley (2005), Long-duration penetration of the planetary electric field to the low-altitude ionosphere during the main phase of magnetic storms, *J. Geophys. Res.*, *110*, A11309, doi:10.1029/2005JA011202.

Kelley, M. C., B. G. Fejer, and C. A. Gonzales (1979), An explanation for anomalous ionospheric electric fields associated with a northward turning of the interplanetary magnetic field, *Geophys. Res. Lett.*, *6*, 301–304, doi:10.1029/GL006i004p00301.

Kherani, A. E., M. Mascarenhas, E. R. de Paula, J. H. A. Sobral, and F. Bertoni (2005), A three dimensional simulation of collisional interchange instability in the equatorial low latitude ionosphere, *Space Sci. Rev.*, *121*, 253–269, doi:10.1007/s11214-006-6158-x.

Kherani, E. A., M. A. Abdu, E. R. de Paula, D. C. Fritts, J. H. A. Sobral, and F. C. de Meneses Jr. (2009), The impact of gravity waves rising from convection in the lower atmosphere on the generation and nonlinear evolution of equatorial bubble, *Ann. Geophys.*, *27*, 1657–1668, doi:10.5194/angeo-27-1657-2009.

Khmyrov, G. M., I. A. Galkin, A. V. Kozlov, B. W. Reinisch, J. McElroy, and C. Dozois (2008), Exploring Digisonde ionogram data with SAO-X and DIDBase, in *Radio Sounding and Plasma Physics*, *AIP Conf. Proc.*, *974*, 175–185, doi:10.1063/1.2885027.

Kikuchi, T., H. Luhr, K. Schlegel, H. Tachihara, M. Shinohara, and T.-I. Kitamura (2000), Penetration of auroral electric fields to the equator during a substorm, *J. Geophys. Res.*, *105*, 23,251–23,261, doi:10.1029/2000JA900016.

Kozlov, A., and V. V. Paznukhov (2008), Digisonde drift analysis software, in *Radio Sounding and Plasma Physics*, *AIP Conf. Proc.*, *974*, 167–174, doi:10.1063/1.2885026.

Kudeki, E., and S. Bhattacharyya (1999), Post sunset vortex in equatorial *F* region plasma drifts and implications for bottom-side spread-F, *J. Geophys. Res.*, *104*, 28,163–28,170, doi:10.1029/1998JA900111.

Le Huy, M., and C. Amory-Mazaudier (2005), Magnetic signature of the ionospheric disturbance dynamo at equatorial latitudes: "Ddyn," *J. Geophys. Res.*, *110*, A10301, doi:10.1029/2004JA010578.

Li, G., et al. (2010), Longitudinal development of low-latitude ionospheric irregularities during the geomagnetic storms of July 2004, *J. Geophys. Res.*, *115*, A04304, doi:10.1029/2009JA014830.

Lin, C. H., A. D. Richmond, J. Y. Liu, H. C. Yeh, L. J. Paxton, G. Lu, H. F. Tsai, and S.-Y. Su (2005), Large-scale variations of the low-latitude ionosphere during the October–November 2003 superstorm: Observational results, *J. Geophys. Res.*, *110*, A09S28, doi:10.1029/2004JA010900.

Mannucci, A. J., B. T. Tsurutani, B. A. Ijima, A. Komjathy, A. Saito, W. D. Gonzalez, F. L. Guarnieri, J. U. Kozyra, and R. Skoug (2005), Dayside global ionospheric response to the major interplanetary events of October 29–30, 2003 "Halloween Storms," *Geophys. Res. Lett.*, *32*, L12S02, doi:10.1029/2004GL021467.

Maruyama, N., et al. (2011), Modeling the storm time electrodynamics, in *Aeronomy of the Earth's Atmosphere and Ionosphere*, *IAGA Spec. Sopron Book Ser.*, vol. 2, chap. 35, pp. 455–464, Springer, New York, doi:10.1007/978-94-007-0326-1_35.

Maruyama, T. (1988), A diagnostic model for equatorial spread *F*: 1. Model description and application to electric fields and neutral wind effects, *J. Geophys. Res.*, *93*, 14,611–14,622, doi:10.1029/JA093iA12p14611.

Maruyama, T., G. Ma, and M. Nakamura (2004), Signature of TEC storm on 6 November 2001 derived from dense GPS receiver network and ionosonde chain over Japan, *J. Geophys. Res.*, *109*, A10302, doi:10.1029/2004JA010451.

Paznukhov, V. V., D. Altadill, and B. W. Reinisch (2009), Experimental evidence for the role of the neutral wind in the development of ionospheric storms in midlatitudes, *J. Geophys. Res.*, *114*, A12319, doi:10.1029/2009JA014479.

Rastogi, R. G., and J. A. Klobuchar (1990), Ionospheric electron content within the equatorial F_2 layer anomaly belt, *J. Geophys. Res.*, *95*(A11), 19,045–19,052, doi:10.1029/JA095iA11p19045.

Reinisch, B. W. (1996), Modern ionosondes, in *Modern Ionospheric Science*, edited by H. Kohl, R. Ruster, and K. Schlegel, pp. 440–458, Eur. Geophys. Soc., Katlenburg-Lindau, Germany.

Reinisch, B. W., and I. A. Galkin (2011), Global Ionospheric Radio Observatory (GIRO), *Earth Planets Space*, *63*(4), 377–381, doi:10.5047/eps.2011.03.001.

Reinisch, B. W., M. Abdu, I. Batista, G. S. Sales, G. Khmyrov, T. A. Bullett, J. Chau, and V. Rios (2004), Multistation Digisonde observations of equatorial spread F in South America, *Ann. Geophys.*, *22*, 3145–3153, doi:10.5194/angeo-22-3145-2004.

Reinisch, B. W., et al. (2009), New Digisonde for research and monitoring applications, *Radio Sci.*, *44*, RS0A24, doi:10.1029/2008RS004115. [Printed 45(1), 2010.]

Richmond, A. D., C. Peymirat, and R. G. Roble (2003), Long-lasting disturbances in the equatorial ionospheric electric field simulated with a coupled magnetosphere-ionosphere-thermosphere model, *J. Geophys. Res.*, *108*(A3), 1118, doi:10.1029/2002JA009758.

Rishbeth, H. (1971), Polarization fields produced by winds in the equatorial *F*-region, *Planet. Space Sci.*, *19*, 357–369, doi:10.1016/0032-0633(71)90098-5.

Rostoker, G., S. I. Akasofu, J. Foster, R. A. Greenwald, Y. Kamide, K. Kawasaki, A. T. Y. Lui, R. L. McPherron, and C. T. Russell (1980), Magnetosphric substorms—Definition and signatures, *J. Geophys. Res.*, *85*(A4), 1663–1668, doi:10.1029/JA085iA04p01663.

Sahai, Y., et al. (2005), Effects of the major geomagnetic storms of October 2003 on the equatorial and low-latitude *F* region in two longitudinal sectors, *J. Geophys. Res.*, *110*, A12S91, doi:10.1029/2004JA010999.

Saito, S., and T. Maruyama (2006), Ionospheric height variations observed by ionosondes along magnetic meridian and plasma bubble onsets, *Ann. Geophys.*, *24*, 2991–2996, doi:10.5194/angeo-24-2991-2006.

Sastri, J. H. (1988), Equatorial electric fields of ionospheric disturbance dynamo origin, *Ann. Geophys.*, *6*(6), 635–642.

Sastri, J. H., M. A. Abdu, I. S. Batista, and J. H. A. Sobral (1997), Onset conditions of equatorial (range) spread *F* at Fortaleza, Brazil, during the June solstice, *J. Geophys. Res.*, *102*, 24,013–24,021, doi:10.1029/97JA02166.

Sastri, J. H., N. Jyoti, V. V. Somayajulu, H. Chandra, and C. V. Devasia (2000), Ionospheric storm of early November 1993 in the Indian equatorial region, *J. Geophys. Res.*, *105*(A8), 18,443–18,445, doi:10.1029/1999JA000372.

Scali, J. L., B. W. Reinisch, C. J. Heinselman, and T. Bullett (1995), Coordinated Digisonde and incoherent scatter radar F region drift measurements at Sondre Stromfjord, *Radio Sci.*, *30*, 1481–1498, doi:10.1029/95RS01730.

Scherliess, L., and B. G. Fejer (1999), Radar and satellite global equatorial *F* region vertical drift model, *J. Geophys. Res.*, *104*, 6829–6842, doi:10.1029/1999JA900025.

Sekar, R., R. Suhasini, and R. Raghavarao (1994), Effects of vertical winds and electric fields in the nonlinear evolution of equatorial spread *F*, *J. Geophys. Res.*, *99*(A2), 2205–2213, doi:10.1029/93JA01849.

Sobral, J. H. A., M. A. Abdu, W. D. Gonzalez, B. T. Tsurutani, and I. S. Batista (1997), Effects of intense storms and substorms on the equatorial ionosphere system in the American sector from ground-based and satellite data, *J. Geophys. Res.*, *102*(A7), 14,305–14,313, doi:10.1029/97JA00576.

Sobral, J. H. A., et al. (2009), Ionospheric zonal velocities at conjugate points over Brazil during the COPEX campaign: Experimental observations and theoretical validations, *J. Geophys. Res.*, *114*, A04309, doi:10.1029/2008JA013896.

Sreeja, V., C. V. Devasia, S. Ravindran, T. K. Pant, and R. Sridharan (2009), Response of the equatorial and low-latitude ionosphere in the Indian sector to the geomagnetic storms of January 2005, *J. Geophys. Res.*, *114*, A06314, doi:10.1029/2009JA014179.

Sutton, E. K., J. M. Forbes, and R. S. Nerem (2005), Global thermospheric neutral density and wind response to the severe 2003 geomagnetic storms from CHAMP accelerometer data, *J. Geophys. Res.*, *110*, A09S40, doi:10.1029/2004JA010985.

Tsunoda, R. T. (2005), On the enigma of day-to-day variability in equatorial spread *F*, *Geophys. Res. Lett.*, *32*, L08103, doi:10.1029/2005GL022512.

Tsurutani, B., et al. (2004), Global dayside ionospheric uplift and enhancement associated with interplanetary electric fields, *J. Geophys. Res.*, *109*, A08302, doi:10.1029/2003JA010342.

Tulasi Ram, S., P. V. S. Rama Rao, D. S. V. V. D. Prasad, K. Niranjan, S. Gopi Krishna, R. Sridharan, and S. Ravindran (2008), Local time dependent response of post sunset ESF during geomagnetic storms, *J. Geophys. Res.*, *113*, A07310, doi:10.1029/2007JA012922.

Valladares, C., and P. H. Doherty (2009), The Low Latitude Ionosphere Sensor Network (LISN), paper presented at 2009 International Technical Meeting of the Institute of Navigation, Anaheim, Calif., Jan.

Wei, Y., M. Hong, W. Wan, A. Du, J. Lei, B. Zhao, W. Wang, Z. Ren, and X. Yue (2008), Unusually long lasting multiple penetration of interplanetary electric field to equatorial ionosphere under oscillating IMF B_z, *Geophys. Res. Lett.*, *35*, L02102, doi:10.1029/2007GL032305.

Zaka, K. Z., A. T. Kobea, P. Assamoi, O. K. Obrou, V. Doumbia, K. Boka, B. J.-P. Adohi, and N. M. Mene (2009), Latitudinal profile of the ionospheric disturbance dynamo magnetic signature: Comparison with the DP2 magnetic disturbance, *Ann. Geophys.*, *27*, 3523–3536, doi:10.5194/angeo-27-3523-2009.

Zhao, B., W. Wan, and L. Liu (2005), Response of equatorial anomaly to the October–November 2003 superstorm, *Ann. Geophys.*, *23*, 693–706, doi:10.5194/angeo-23-693-2005.